15

Primary Bone Tumors

Robert Howman-Giles, Rodney J. Hicks, Geoffrey McCowage, and David K. Chung

Musculoskeletal sarcomas represent a heterogeneous group of malignancies involving bone and soft tissue with a highly variable natural history and a correspondingly diverse range of potential therapeutic strategies. The choice of treatment is largely driven by prognostic factors but is also dependent on local expertise, resources, and philosophies and the particular clinical circumstances of individual patients. Important considerations include the type, grade, extent, and location of the tumor. Curative treatment approaches in osteogenic sarcoma combine surgery and chemotherapy. In Ewing sarcoma, chemotherapy is used, and local control is achieved by surgery, radiotherapy, or a combination of both (1–3).

This chapter focuses on primary bone tumors in the pediatric population with an emphasis on the two most common forms: osteogenic sarcoma (OS) and Ewing sarcoma (ES). An initial general clinical summary provides the setting for understanding the role of diagnostic imaging in their assessment and management. The current contribution of positron emission tomography (PET) is summarized with an outline of likely future developments that promise to expand its range of applications.

Epidemiology

Primary bone tumors make up 5% to 6% of childhood malignancy, and the overwhelming majority of cases consist of either OS or ES (4–7). Other conditions more common in the pediatric than the adult population are Langerhans cell histiocytosis and primary bone lymphoma; however, collectively these account for a small percentage of primary malignant bone tumors. A smaller number of patients have other diagnoses such as malignant fibrous histiocytoma, angiosarcoma, and chondrosarcoma, but these conditions are very rare in the pediatric age group. The age distribution of patients with bone tumors is different from most other forms of childhood cancer. Childhood leukemia and solid tumors such as neuroblastoma, Wilms' tumor, and soft tissue

sarcomas have their peak incidence during the first decade. In contrast, both OS and ES are more common in the second and third decades, a period in life also associated with accelerated normal bone growth.

Osteogenic sarcoma is a rare cancer arising from bone matrix and affecting children and adolescents. There is no sex or race predilection; in the United States the incidence is estimated to be 2 to 3 per million people. Most cases of OS (approximately 80%) occur between the ages of 5 and 25 years. Primary OS characteristically occurs in the metaphyseal regions of the long bones of the extremities, most frequently the distal femur, proximal tibia, and proximal humerus. Approximately 55% arise near the knee, but any bone can be affected including the flat bones and axial skeleton (4,6). Osteogenic sarcoma is usually a primary bone malignancy, but secondary forms may arise from Paget's disease, fibrous dysplasia, and multiple chondromas. These secondary forms are generally confined to older individuals and are not relevant to the pediatric population. There is also an association with previous radiation therapy, with the majority of cases in this group appearing within 7 to 15 years after the therapy. Again, this is usually beyond the pediatric period. There is, however, an association with bilateral retinoblastoma that is relevant to pediatric patients. Outcome is usually poor in all these secondary forms of OS (6).

Ewing sarcoma is a rare tumor arising from mesenchymal origin. It is the second most common malignant bone tumor after OS. It most commonly occurs in the second decade, with a peak age range from 4 to 15 years. The frequency in the United States ranges from 0.3 per million for children <3 years to 4.6 per million in patients aged from 15 to 19 years. Males are affected more frequently than females with a ratio of 1.5:1. Ewing sarcoma is most common in the white population and is rare in black and Chinese children. It most frequently involves the pelvis (25%), femur, tibia and fibula, spine, ribs, and humerus. Any bone may be involved (5,7).

Presentation

The most common presenting symptom for primary bone tumors is a painful swelling arising in bone. Pain is often initially attributed to trauma or physical exercise; symptoms may be present for several weeks or even months before diagnosis. The pain may be intermittent and severe, usually with a palpable mass, which is rapidly growing and often tender. There may be referred pain to the limbs if the primary is in the axial skeleton or pelvis. There may also be pain related to nerve root or cord compression if there is spinal involvement. Occasionally the patient may present with a pathologic fracture. The presentation may be similar to acute or chronic osteomyelitis with systemic symptoms of fever, malaise, weight loss, and leukocytosis. The majority of patients do not have clinical evidence of metastatic disease, but most are thought to have microscopic metastases, undetectable by conventional imaging techniques, at the time of presentation. Approximately 15% to 20% of patients have clinically evident metastatic disease at

diagnosis. The lungs are the most common site of metastases, followed by bone and bone marrow (4,5).

Although imaging studies may be highly suggestive of the diagnosis of primary bone tumors, they cannot reliably differentiate among the various types of malignant bone tumor and occasionally cannot differentiate between malignant and benign conditions. Histopathologic confirmation, therefore, is required. Other differential diagnoses based on radiologic appearances can include infection (particularly destructive osteomyelitis), which may be very difficult to differentiate from malignancy, particularly in some areas such as the sacroiliac joint and vertebrae, and other bone malignancies including bone metastases and primary lymphoma of bone (4–8).

The treatments for OS and ES have much in common, in particular the routine use of neoadjuvant chemotherapy and the role of surgery. Radiotherapy has an important role in ES, particularly if the primary tumor cannot be surgically resected. There are, however, important differences in the approach to management of these two tumors. Knowledge of tumor histology, grade, and the presence or absence of metastases are the main prerequisites for allowing appropriate treatment selection. The other major factor that influences treatment and prognosis is the tumor response to therapy (9–11).

As these tumors are very heterogeneous in nature, the sites for biopsy are critical for accurate histologic staging. Biopsy of a small site of a tumor may not represent the overall character of the tumor and has the potential to miss high-grade areas (12). The implications of this are errors in diagnosis and grading that could influence the type of treatment given (13–15). Nondiagnostic biopsies may also occur, necessitating repeat biopsy. This may increase the risk of biopsy track seeding and may complicate the subsequent surgical technique. Open biopsy yields larger tissue samples for analysis and is generally preferable to core-needle biopsy. However, in experienced units, core biopsy can be a reliable technique and can expedite diagnosis because operating room time is not required. When planning biopsy, the nature of planned subsequent definitive surgery needs to be considered so that the biopsy site and tract can be included in the final resection. Resection at diagnosis is rarely performed, as delayed resection after neoadjuvant chemotherapy is now routine initial management of primary bone tumors (8).

Metastatic spread is mainly hematogenous initially to the lungs and later skeleton and bone marrow, although spread via the lymphatic system may occur. If local recurrence occurs, it is often difficult to diagnose as there is disturbance of the normal anatomic structures due to previous surgery or radiotherapy and imaging can be difficult to interpret due to artifacts from limb prostheses (8,13).

Histopathology

The diagnosis of malignancy involving bone requires histopathologic confirmation. Histopathology of OS reveals malignant sarcomatous tissue composed of pleomorphic spindle cells admixed with an

extracellular matrix composed primarily of osteoid and bone. Such osteoid is an absolute requirement for the diagnosis of OS to be made, although occasionally osteoid is present only in small amounts, making the diagnosis difficult. Conversely, in the presence of pathologic fracture, immature osteoid can mimic OS. A number of histologic subtypes of OS exist, each with characteristic pathologic features. The most common subgroup is conventional OS, which is further divided into osteoblastic, chondroblastic, or fibroblastic variants, depending on the dominant pattern of differentiation of tumor cells. Other subgroups are telangiectatic, small cell, multifocal, periosteal, and parosteal OS. Most of these subtypes have similar clinical behavior, and management is similar except for the parosteal variant, which is more common in older patients, is typically of low histopathologic grade, and is associated with a more indolent clinical course (4,6).

Ewing sarcoma, peripheral neuroepithelioma, and primitive neuroectodermal tumor (PNET) belong to the Ewing family of tumors. Ewing sarcoma derives from a primitive neuroectodermal cell with variable differentiation. It is a poorly differentiated small, round, blue cell tumor where PNET shows discernible differentiation. All these tumors show some neural differentiation and have neural features, including expression of neuron specific enolase and S-100 protein. Both show a characteristic chromosomal translocation t(11; 22) or a variation within the tumor cell (5,7).

Diagnostic Imaging of Primary Bone Tumors

Anatomic imaging techniques including radiography, ultrasound, computed tomography (CT), and magnetic resonance imaging (MRI) currently play a dominant role in the evaluation of suspected and known sarcomas of both soft tissue and bone. Nuclear medicine techniques such as bone scintigraphy, thallium-201 (^{201}TI), and gallium-67 (^{67}GA) imaging have all been used in the assessment of primary bone tumors. However, PET is becoming the most important modality for assessing biologic characteristics of the tumor, for primary staging, and for determining response to treatment (13,16–18).

The diagnosis of primary bone tumor is usually made on a plain radiograph but may be suspected based on clinical examination findings. Osteogenic sarcoma is usually seen as an expansile, destructive lesion but may be sclerotic, lytic, or a combination of both. There is usually a significant degree of new bone formation. Often bone spicules are present running perpendicularly to the surface or arranged radially as a "sunburst" pattern. This is typical of the most common osteoblastic form of OS. There is usually a poorly defined zone of transition to normal bone that may be associated with a soft tissue mass. Lifting of the bone's normal periosteum by tumor may lead to the formation of Codman's triangle (6,19). The local extent, intramedullary spread, and relationship to soft tissue structures, particularly the neurovascular bundle, is best detected by cross-sectional imaging, in particular, by MRI.

In ES conventional radiology shows an aggressive destructive tumor with a permeated or moth-eaten appearance—a predominantly lytic lesion with poorly defined margins. The lesion is usually diaphyseal or metaphyseal with a soft tissue mass. There may be saucerization of the bone and a lamellated periosteal reaction with an onionskin pattern. There may be a spiculated pattern of new bone formation, which can be confused with the more common OS. Sclerotic lesions occur in approximately 25% of cases. There may be invasion of cortical bone, or the cancer may traverse the Haversian system and cause a large soft tissue mass in the absence of significant bone destruction. Based on the variable patterns observed radiologically, the differential diagnosis can include infection, OS, chondrosarcoma, fibrosarcoma, soft tissue sarcoma, and Langerhans cell histiocytosis. Lymphoma and leukemia may also mimic ES radiologically (7,19).

Magnetic resonance imaging and CT scanning allow definition of intralesional structural characteristics and of the relationship between tumor boundaries and adjacent normal tissues, including bone and neurovascular structures. For this purpose, MRI is now the major diagnostic tool (19,20). Regional anatomic information is important to determine the need for and approach to biopsy and to guide subsequent locoregional therapies, including radiotherapy and surgery. Tissue heterogeneity can make problematic the selection of the most appropriate biopsy site and the interpretation of anatomic imaging results following therapy. This is an important potential limitation because the behavior of sarcomas, their prognosis, and determination of the most appropriate management are influenced by the highest histologic grade of tumor that is present (12,21,22). Furthermore, for staging purposes, sensitive and specific whole-body screening capability is required.

Metastatic spread usually occurs first to the lungs and then to the skeleton. Computed tomography scan of the thorax is the main imaging modality for detection of pulmonary metastases, and the radionuclide bone scan is currently the primary investigation to detect skeletal metastases (4,5). Combined PET/CT imaging, however, is becoming the preferred modality for the detection of metastatic spread because of its ability to detect both soft tissue and bone sites of disease (Fig. 15.1), whereas the contemporaneous CT maintains good sensitivity for small lung metastases.

Treatment

The overall plan of management for localized primary bone tumor generally involves administration of preoperative neoadjuvant chemotherapy, delayed tumor resection and/or radiotherapy, and then further chemotherapy (8). The choice of postoperative chemotherapy is often dependent on the degree of tumor necrosis documented in the resection specimen on comprehensive histopathologic examination (11,13). Neoadjuvant chemotherapy is routinely used for several reasons:

- Chemotherapy treats micrometastatic disease, which is believed to be present but undetectable in many cases.

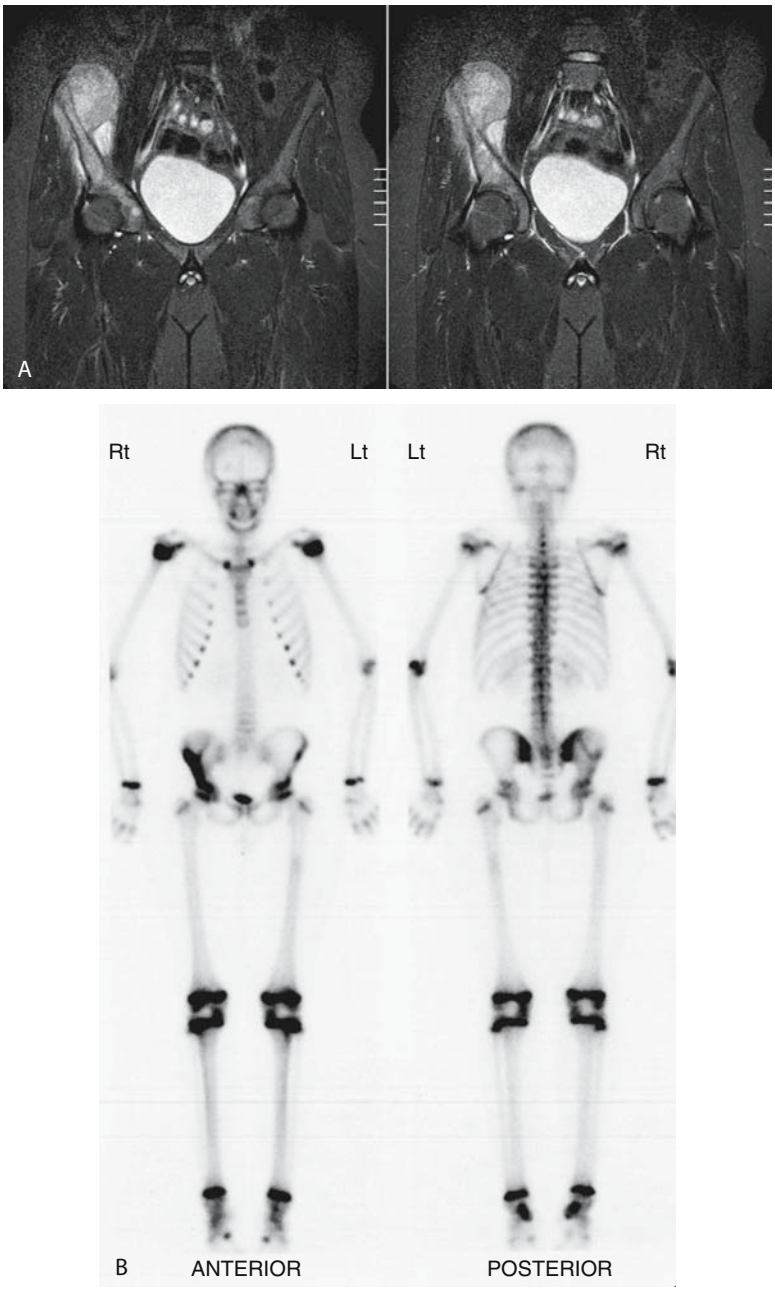

Figure 15.1. Pelvic Ewing sarcoma with bone metastases. A: A 13-year-old boy presented with a painful right hip. Magnetic resonance imaging (MRI) [short time inversion recovery (STIR) sequence coronal views] shows a primary pelvic tumor in the right iliac wing with a large soft tissue mass. B: Technetium-99m (^{99m}Tc) methylene diphosphonate (MDP) total bone scan shows a right pelvic primary tumor with marked osteoblastic reaction and metastatic sites in left mid-femur and sacrum. No other sites were detected. C: Fluorine-18 fluorodeoxyglucose (^{18}F-FDG) scan shows primary tumor and multiple metastases in the bone and marrow, particularly in the spine and pelvis. The patient initially responded to chemotherapy and radiotherapy to the primary tumor. Follow-up positron emission tomography (PET) showed good response with only a mild uptake of FDG in the primary site. The patient subsequently relapsed with metastases in the bone on PET (not shown).

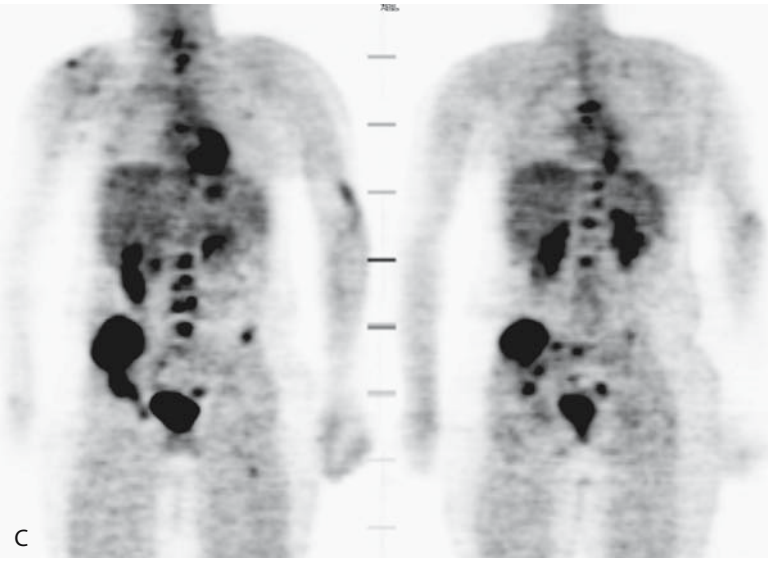

Figure 15.1. *Continued.*

- Resolution of soft tissue masses using chemotherapy may facilitate subsequent surgery.
- The period of some weeks between diagnosis and surgery allows for the ordering of customized orthopedic components such as prostheses or bone allografts that will be used at the time of surgical resection and limb reconstruction.
- Valuable information is obtained regarding the sensitivity of the tumor to the neoadjuvant chemotherapy agents. Patients with tumors that have a good histopathologic response to these drugs are given similar therapy postoperatively, whereas alternate agents and external beam radiotherapy may be considered if the tumor response has been poor.

After neoadjuvant chemotherapy but prior to surgery, imaging studies are repeated to evaluate tumor response and to exclude the development of new metastatic disease that might make aggressive surgery inappropriate. In particular, detection of metastases significantly reduces the chance of disease-free survival and usually argues against aggressive surgery on the primary unless the number of metastatic sites is small and also amenable to surgical resection.

Surgery in OS generally takes the form of a limb salvage procedure (4,23,24). The data show that the overall survival rate with such procedures approximates that obtained using amputation, but the functional outcome is superior. There is a higher risk of local recurrence (13,25,26), so effective multidrug chemotherapy is mandatory to prevent it. Similarly, in ES where historically radiotherapy was used for local control and surgery was used primarily for expendable bones, limb salvage surgery following chemotherapy is now the treatment of choice if the tumor can be completely removed and the function after

surgery is predicted to be reasonable. The preference for surgery when possible in ES is largely due to the late effects of radiotherapy, especially second malignancy. In both cancers, radical tumor resection is performed if possible, followed by some form of reconstructive procedure using a prosthetic component, bone autograft or allograft, or more complex procedures, for example, rotation arthroplasty.

Histopathologic response is particularly important in primary bone tumors because lower "cell kill" is associated with an inferior prognosis (25). Alternate chemotherapy agents may be applied in such settings. Where there has been a good histologic response, similar agents are used postoperatively as were used at diagnosis, for a total treatment duration of 5 to 12 months (8).

Following completion of chemotherapy, most patients undergo some form of periodic screening for detection of recurrence and metastatic disease. Protocols vary but usually include chest x-ray, chest CT, imaging of the primary site with MRI or CT, and radionuclide bone scan. Fluorodeoxyglucose (FDG)-PET is having increasing application in this area.

Recurrent disease following therapy is a grave development, and only a small minority of such patients survive their disease. Restaging by imaging may be vital in facilitating timely diagnosis of recurrence and thereby improving the poor prognosis of such patients. Positron emission tomography has a major role in restaging. Therapeutic options for recurrent sarcoma include surgery, further chemotherapy, and palliative radiation therapy. Patients who develop isolated pulmonary metastases may be candidates for thoracotomy and metastasectomy; occasionally multiple such procedures can provide prolonged disease control. Recurrence at the primary site may require amputation. Further chemotherapy options may be limited because recurrence implies that there is drug resistance to the original agents. Such patients are candidates for experimental drug trials using novel agents.

Prognosis

The best predictor of outcome for patients with primary bone tumors without evidence of metastatic disease is the histologic response to induction chemotherapy (Figs. 15.2 and 15.3). This assessment is usually made at the time of surgery after neoadjuvant chemotherapy (4,5,25). A method to noninvasively assess treatment response would be very useful, as nonresponding tumors may require alternative or additional chemotherapy prior to their definitive surgery. Patients with OS that is localized at diagnosis have a relatively good prognosis: approximately 55% to 75% of such patients can be expected to be cured permanently. Patients with metastatic disease have an event-free survival below 20% (4). For ES, the European Intergroup Cooperative Ewing's Sarcoma Study (EICESS) reported the 3-year event-free survival rate was 66% in patients with localized tumors, 43% in those with lung metastases at initial diagnosis, and 29% in those with other metastases. A large tumor volume and a tumor primarily localized to the pelvic area were also negative prognostic factors (5).

Positron Emission Tomography

Positron emission tomography (PET) is an exciting technology for cancer evaluation, combining relatively high spatial resolution with high lesion contrast and the ability to assay biologic processes throughout the body. The commonest PET tracer used is fluorine-18 fluorodeoxyglucose (FDG). New hybrid PET-CT devices provide further enhancement of the potential of this modality by allowing accurate coregistration of functional and anatomic information, improving the localizing ability of PET (27).

The improved management and outcomes for primary bone tumors relate to improved diagnostic methods and to more reliable staging of the disease, which allows more appropriate treatment with both neoadjuvant chemotherapy and more patient-specific surgical procedures. Positron emission tomography is having increasing application as an additional modality to conventional imaging for more accurate tumor staging and restaging. This relates to primary tumor localization and extent, including soft tissue local disease, intramedullary extension, and detection of metastatic disease. It is also becoming the preferred modality to determine tumor response to neoadjuvant therapy. Therefore, PET has a major impact on the selection of appropriate chemotherapy regimens, surgical procedures, and prognosis (13,17,18).

Positron emission tomography imaging entails not only improved sensitivity for detecting malignant lesions but also quantitative procedures to be applied in the evaluation of primary bone tumors. The usual methods for quantitation are standard uptake value (SUV), tumor-to-background ratios (T/BG), graphical analysis, and nonlinear regression analysis based on a three-compartment model (13). These methods can generally be applied in the evaluation of primary bone tumors. In some cases, lack of significant blood pool–containing structures in the imaging field of view limits image-based evaluation of the arterial input function of radiotracer and may require arterial blood sampling. For practical reasons, most clinical studies have utilized SUV calculation rather than compartmental modeling or other quantitative approaches.

Initial Imaging of Primary Tumor

Tumor Grading

Many publications indicate that as the degree of FDG uptake is a measure of metabolic activity, it is indicative of tumor grade, that is, aggressiveness. The early studies using PET in musculoskeletal tumors in primarily adult populations showed increased uptake of FDG. The highest uptake of FDG was found in high-grade tumors, both soft tissue sarcomas and OS, when compared to low-grade or benign tumors (28–30). Subsequent publications have confirmed this finding. There is a significant correlation of histologic grading or tumor aggressiveness with FDG uptake measured by T/BG ratio, SUV, or kinetic modeling techniques (Table 15.1). Eary et al. (12) reported that tumor FDG uptake expressed as maximum SUV (SUV_{max}) has a high

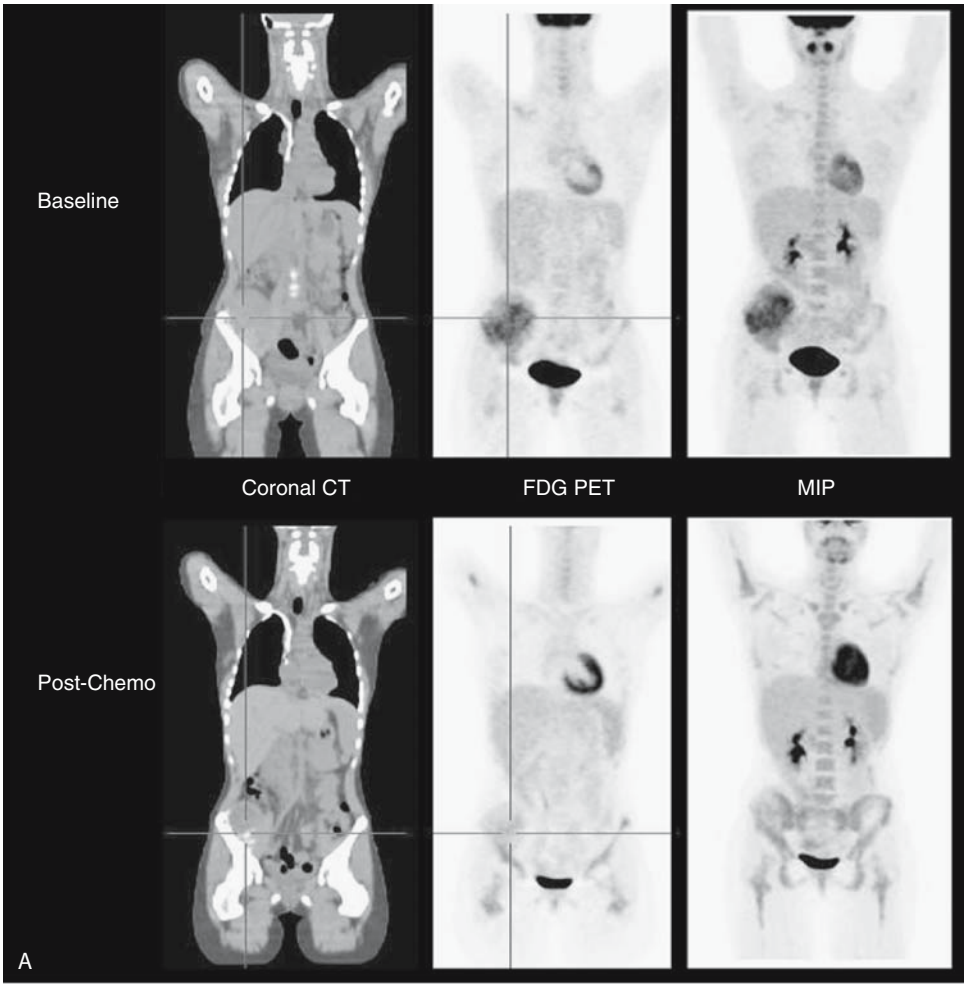

Figure 15.2. A good response to treatment. A: Ewing sarcoma. Images obtained on a combined PET–computed tomography (CT) of a large Ewing sarcoma of the pelvis with an extensive soft tissue mass at baseline (above) and after three cycles of chemotherapy (below). CT demonstrated negligible change, but a significant reduction in metabolic signal was apparent in both the osseous and soft tissue components, indicating a favorable response to treatment. The maximum intensity projection (MIP) images demonstrate relatively increased bone marrow activity following treatment. This is a common finding following chemotherapy and is thought to represent activated bone marrow. The changes are more pronounced with the use of growth factor (e.g., granulocyte colony-stimulating factor, G-CSF) support, but in children they can be very prominent even without this growth factor. B: Osteogenic sarcoma. Sequential coronal planes at baseline (above) and following completion of chemotherapy (below) demonstrate normal physiologic uptake of radiotracer in the epiphyseal growth plates of the right knee. A slightly heterogenous lesion with high FDG avidity is present on the baseline study in distal left femur that clearly crosses the growth plate to involve the epiphysis. On the posttreatment scan there is only low-grade peripheral uptake and no residual FDG uptake epi-centered on the initial sites of tumoral involvement. This was classified as a complete metabolic response and had >98% necrosis on the excision pathology specimen. C: From the same case displayed in B, MIP images demonstrate the change in biodistribution of FDG at baseline (left) and after chemotherapy (right). Normalizing the images to liver, which generally has the highest basal utilization of glucose of normal soft tissues under fasting conditions, demonstrates a marked reduction in uptake in the primary tumor but a marked increase in bone marrow activity. The posttreatment scan (performed during winter) also demonstrated significant uptake in cervical, axillary, paravertebral, and peridiaphragmatic brown fat. Despite the lack of significant CT response, the transaxial reference images (below) demonstrate a very significant reduction in tumoral FDG uptake. In the posttreatment setting, it is common to have a very homogeneous rim of low-grade uptake around the periphery of the initial tumoral site. This correlates with the development of an inflammatory pseudocapsule. We do not interpret this as residual tumor and classified this as a complete metabolic response. Partial metabolic responses are usually characterized by residual FDG that is epi-centered within areas of previous tumoral uptake rather than being peripheral to them.

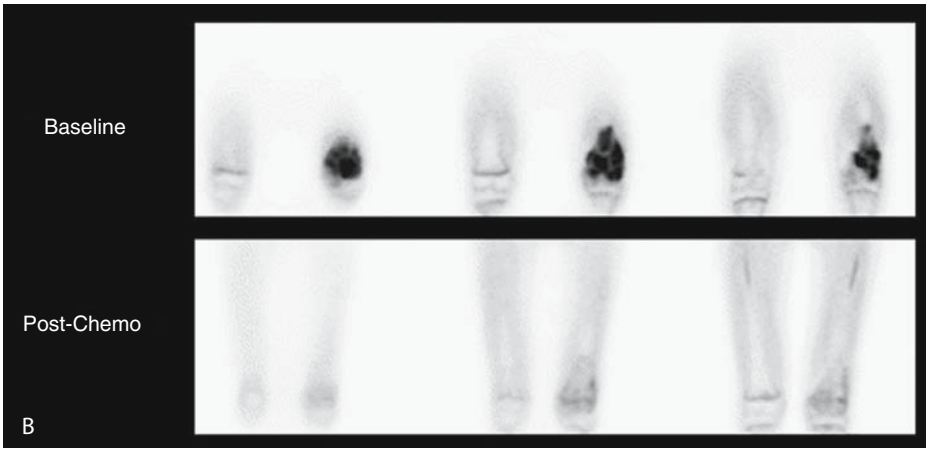

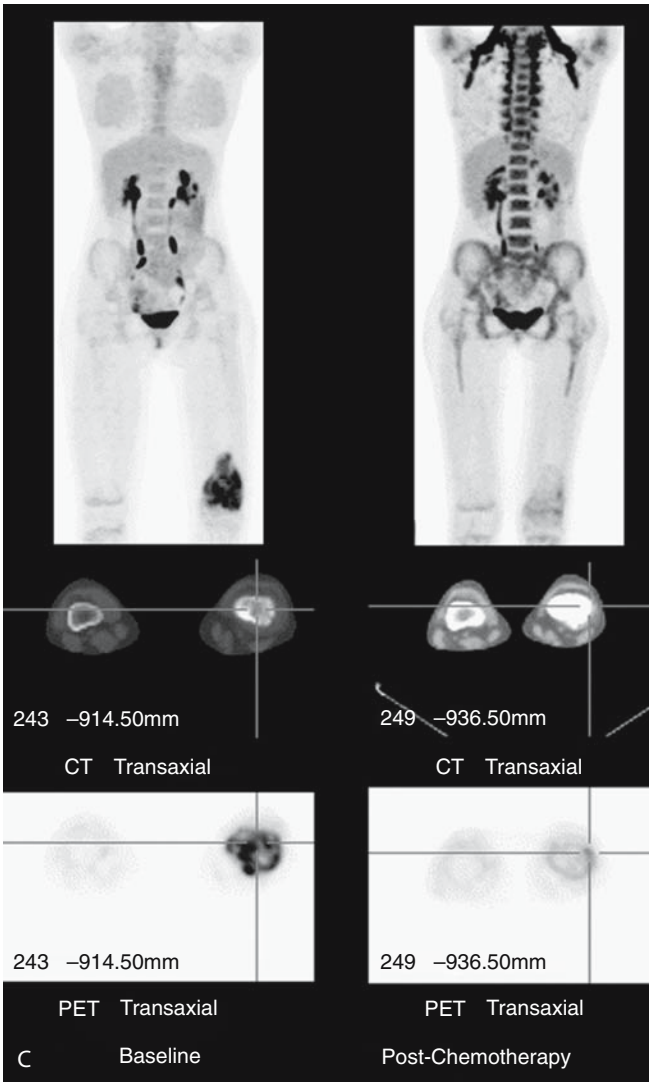

Figure 15.2. *Continued.*

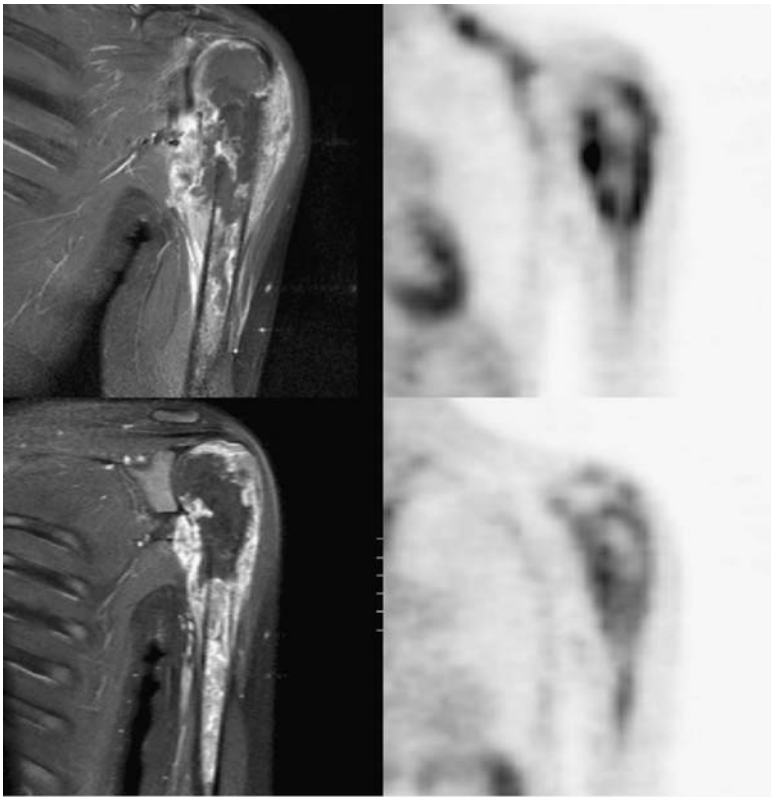

Figure 15.3. A poor response to treatment. Osteogenic sarcoma of the proximal left humerus in a 14-year-old girl. Top row shows pretherapy MRI (T1 postgadolinium) and ^{18}F-FDG study. The MRI shows marked destruction of the proximal humerus with tumor crossing the growth plate, central bone necrosis, and extensive soft tissue tumor mass. The PET study shows marked heterogeneous distribution of FDG in the proximal humerus with focal increased metabolism seen peripherally and central necrosis. This scan indicates more specific biopsy sites in the most metabolic areas. This patient was a poor responder to neoadjuvant therapy (bottom row), with the MRI showing significant enhancement and the PET study persisting increased uptake. The postsurgical resection specimen showed <5% necrosis confirming poor response. Subsequently, this patient developed pulmonary metastases.

correlation with tumor grade in a series of 42 patients with soft tissue and bone sarcoma. Specific types of bone tumor were not detailed. The same group reported that the median SUV_{max} was significantly different for each histologic grade of tumor when divided into high-, intermediate-, and low-grade tumors. Looking at other markers of tumor aggressiveness, such as increased tumor cellularity, mitosis, and level of Ki-67 (proliferation of a specific nuclear antigen detected by immunohistochemical staining which correlates with growth fraction of tumors) proliferative index, there was also a significant correlation found with SUV_{max}. These researchers and others have also found moderate correlation with tissue levels of the cell growth regulation product p53 (31,32). These parameters have been correlated with a poorer outcome for higher tumor grades, shorter survival, and development of distant metastatic disease.

Table 15.1. Summary of studies of histologic grading or tumor aggressiveness and measures of fluorodeoxyglucose uptake

Study	No. of patients and tumor type	Histologic grade good	Overlap malignant vs benign	SUV T/NT	SUV malignant	SUV benign	Mit cell Ki-67	Sensitivity	Specificy	Accuracy	Survival SUV high
Eary et al. (12)	70 ST and BS	Yes									Yes
Schulte et al. (33)	202; 44 OS, 14 ES	Yes	Yes	T/NT >3.0	T/BG 3.3–73* T/BG 1.4–31.0**	T/BG 3.0–35.0		93%	67%	82%	
Feldman et al. (34)	45 ST and BS, 24 BS, 3 OS, 1 ES	Yes	Yes	SUV_{max} >2.0	SUV_{max} 3.74–9.23	SUV_{max} 0.81–1.74		92%	100%	92%	
Dimitrakopoulou-Strauss et al. (35)	83; 9 OS, 8 ES	Yes		SUV + dynamic indices	SUV_{max} 3.7 (0.4–12.3)	SUV_{max} 1.1 (0.4–3.5)		SUV 54% SUV + dynamic 76%	91% 97%	75% 88%	
Aoki et al. (36)	52; 6 OS, 2 ES	Yes	Yes	SUV_{mean}	SUV 4.34 ± 3.19	SUV_{mean} 2.18 ±1.52					
Kole et al. (38)	26; 5 OS, 2 ES	No	Yes large	SUV_{av} MRFDG SUV_{max}	SUV_{av} 3.2 (0.74–7.64) SUV_{max} 7.07 (2.23–16.06)	SUV_{av} 0.53 (0.22–1.07)					
Eary et al. (31)	209; 52 BS	Yes			SUV_{max} 1.4–60.0		Yes				Poor
Franzius et al. (39)	29 OS	Yes		T/NT_{avg} 4.5 T/NT_{max} 12.6							T/NT_{max} poor
Folpe et al. (32)	89 ST and BS	Yes					Yes				Poor

*High grade sarcoma

**Low grade sarcoma

BS = Bone sarcoma; ES = Ewing sarcoma; Mit Cell Ki67 = correlation SUV with indices of tumor aggressiveness (i.e. mitotic activity, cellularity, Ki67); OS = osteogenic sarcoma; Overlap = between malignant and benign. Some benign may have high uptake; ST = soft tissue; SUV_{av} = SuVaverage; T/NT = Tumor uptake/Nontumor uptake.

Schulte et al. (33) used T/BG ratios in their series of 202 patients, including 44 patients with OS and 14 with ES. Among the bone sarcomas, OS had a tendency to higher T/BG ratios than did ES. Glucose metabolism was greater for high-grade malignant lesions than for low-grade tumors. Using a T/BG ratio of >3.0 for malignancy, the sensitivity was 93%, specificity 66.7%, and accuracy 81.7%. Other authors have used cutoff values of SUV to help differentiate between malignant and benign bone lesions. Feldman et al. (34) reported using a SUV_{max} cutoff of 2.0 for differentiating malignant from benign osseous and nonosseous lesions. They reported a sensitivity of 91.7%, specificity of 100%, and accuracy of 91.7%. All aggressive lesions had a SUV_{max} of >2.0. The differentiation was significant statistically. Dimitrakopoulou-Strauss et al. (35) reported dynamic quantitative FDG-PET in 9 OS and 8 ES patients in a group of 83 patients. Malignant tumors showed enhanced uptake, but there was visually an overlap with some benign lesions. The mean SUV was 3.7 (range 0.4–12.3) for malignant tumors compared to 1.1 (range 0.4–3.5) for benign lesions. Two grade I OS, one grade I ES, and a neuroectodermal tumor did not show enhanced FDG uptake. The authors used other parameters that also showed higher values in malignant tumors compared to benign lesions, but there was some overlap. They reported a sensitivity of 76%, specificity of 97%, and accuracy of 88%. Aoki et al. (36) in 52 patients showed a significant difference in the mean SUV between benign and malignant bone conditions. Although OS had high SUV, there were several other conditions, in particular giant cell tumors, fibrous dysplasia, sarcoidosis, and Langerhans cell histiocytosis, that also had high values. A cutoff level for differentiating OS could not be applied. Other benign or nonmalignant conditions that may have high FDG uptake and high SUV values are infective or inflammatory conditions such as osteomyelitis. Watanabe et al. (37) could not differentiate between osteomyelitis and malignant bone tumors. Also of note in their group of patients was that skeletal metastases tended to have higher SUV values than primary OS.

Only one publication reported no correlation between metabolic rate of glucose metabolism and biologic aggressiveness of bone tumors. Kole et al. (38) described 19 malignant and seven benign tumors. All lesions were clearly visualized by FDG-PET except for an infarct in a humerus. When SUV and Patlak derived metabolic rates were used to try to differentiate between benign and malignant tumors, there was a wide overlap between patients. The authors also commented that patients with low metabolic rates had a poor response to chemotherapy, and one patient with high rate responded well. They also observed that malignant fibrous histiocytoma and lymphoma had high rates compared to OS.

Indication of Prognosis

The prognostic value of PET may be even more important than its ability to define histopathologic grade. Eary et al. (31) analyzed SUV_{max} for the ability to predict patient survival and disease-free survival. In

a retrospective analysis of 209 patients with sarcoma (52 primary bone tumors) who had FDG-PET, a multivariate Cox regression analysis was applied to SUV_{max} in predicting time to death or disease progression. The authors stated that SUV_{max} is a significant independent predictor of patient survival and disease progression. Tumors with higher SUV_{max} had a significantly poorer prognosis. Also, SUV_{max} had better correlation for histologic tumor grades with a higher significance of baseline SUV for prediction of outcome compared to conventional tumor imaging. Franzius et al. (39) evaluated 29 patients with primary OS. Using the average and maximum tumor-to-nontumor ratios (T/NT), they determined there were prognostic implications for OS based on the degree of FDG uptake. After chemotherapy, the patients underwent surgery, and response was determined histologically. Both overall and event-free survival were significantly better in patients with low T/NT_{max} than in patients with high T/NT_{max}. It was concluded that the initial glucose metabolism of primary OS, as measured by FDG T/NT_{max}, clearly discriminated between those patients with a high probability of overall and event-free survival versus OS patients with a poor prognosis. Of note was the fact that no significant difference was found between the various OS histology subtypes or the different regression grades. There was also no significant difference between the size of the primary tumor and uptake values. The fact that high FDG uptake correlates strongly with a poor outcome despite imperfect correlation with other known prognostic factors suggests that it may reflect a number of disparate adverse biologic characteristics.

Local Extent of Primary Tumor

Conventional cross-sectional radiographic imaging, that is, MRI and CT, are routinely used to define both the intraosseous and extraosseous extent of the primary tumor (Figs. 15.1 and 15.2). However, PET adds further information to these cross-sectional techniques, particularly with respect to intramedullary extension and skip lesions. Magnetic resonance imaging may overestimate tumor extension due to signal abnormalities of peritumoral edema. Also changes within the marrow cavity may be considered abnormal in children but may be due to physiologic red blood marrow distribution (40). Other changes such as necrosis or fibrosis within the tumor can be characterized better with PET.

Biopsy and Sampling Error

Histopathologic classification is a vital step in the management of suspected sarcomas. Tumor grade determined from biopsy has significant prognostic and management implications. The ability of PET to determine the biologic aggressiveness of tumors is very useful in indicating which sites in a tumor should be biopsied. There is usually marked heterogeneity of FDG uptake in sarcomatous tumors, and the accuracy of tumor diagnosis and the histologic grading may suffer from poor sampling. The areas of high metabolic activity are often seen

in the peripheral regions of the tumor mass, particularly in large heterogeneous tumors within which there may be large areas of necrosis. False tumor grading, particularly an erroneous assessment of low grade, could have a significant impact on appropriate chemotherapeutic options. Folpe et al. (32) reported a good differentiation between levels of tumor grading by PET but could not distinguish between grade II and grade III tumors. Also, other tumors and some benign tumors may have high SUV values. Currently the published data do not support the idea that biopsy can be avoided as there are different histologic types of bone tumors that will determine specific treatments and there can be an overlap of some benign conditions. As the higher grades of tumor determine the overall histologic tumor grade and therefore predict outcome, the application of PET to indicate the most metabolically active sites of the tumor (Fig. 15.3) should allow better and more accurate sampling of the tumor (13,18).

False Positives

Fluorodeoxyglucose-PET has been reported to show increased accumulation in other malignant tumors, and in benign, inflammatory, and infective lesions. These include giant cell tumor, fibrous dysplasia, Langerhans cell histiocytosis, chondroblastoma, chondromyxoid fibroma, desmoplastic fibroma, aneurysmal bone cyst, nonossifying fibroma, fracture (Fig. 15.4), simple bone cyst with fracture, acute and chronic osteomyelitis, and renal osteopathy (13,33). These conditions generally require a positive diagnosis, if only for purposes of reassur-

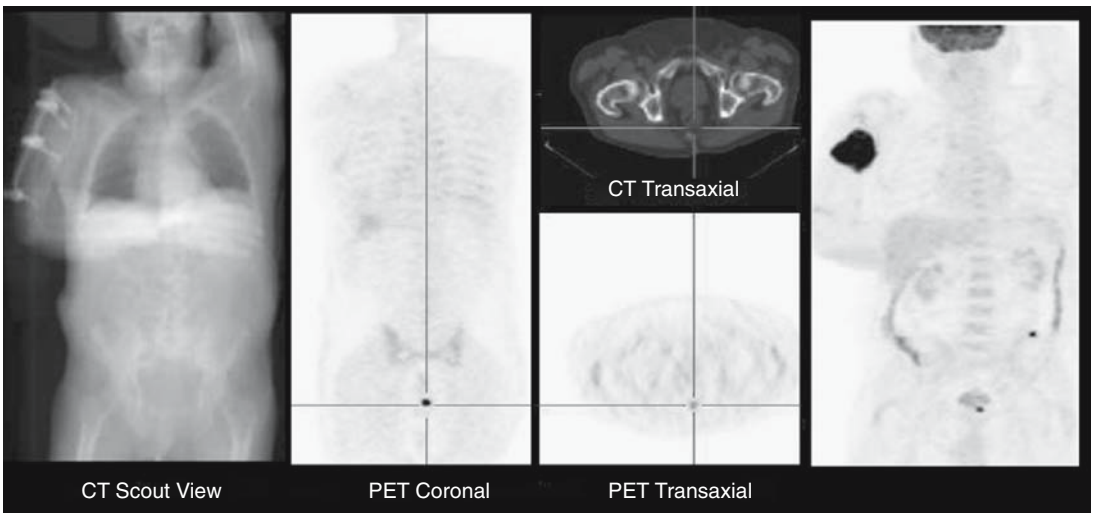

Figure 15.4. False-positive PET from a pathologic fracture. Although not a pediatric case, this figure illustrates the difficulty that can arise in differentiating between a pathologic fracture and primary osteosarcoma of bone. Based on clinical presentation and a biopsy taken at the time of internal fixation, this patient was believed to have an osteosarcoma of the right humerus. A staging PET scan demonstrated focal uptake in the prostate, and metastatic prostate cancer was subsequently confirmed on further immunohistochemistry of the initial biopsy specimen.

ance, and may have specific treatment that can be delivered once a diagnosis has been reached. Accordingly, these false-positive results need to be considered in the clinical context in which they occur. Certainly, if they were to lead to unnecessary or inappropriate surgery or chemotherapy, these results would be considered undesirable, but if they help to guide biopsy or exclude additional sites of disease, they can make a valuable contribution to patient management.

Metastatic Disease

In approximately 20% of cases there are clinically detectable metastases at diagnosis.

Pulmonary

As the main metastatic spread is to the lungs initially, high-resolution spiral CT (HRCT) is the recommended investigation. Since the implementation of the HRCT technique, there has been a doubling of detection of pulmonary metastases (10,13). Localized areas of pulmonary metastatic disease may be amenable to surgical removal. Positron emission tomography scans are useful to exclude additional macroscopic disease beyond the lungs. In some cases PET can also reliably identify false-positive results on CT and thereby spare patients unnecessary thoracotomy.

Schulte et al. (41) performed a comparison of CT and PET in detecting pulmonary metastases but did not show any significant difference for the number of lesions. Other studies have reported similar findings in soft tissue sarcoma. However, Franzius et al. (42) reported a comparison of CT and PET for pulmonary metastases in 32 patients who had 49 PET scans. The sensitivity, specificity, and accuracy of FDG-PET were 50%, 100%, and 92%, respectively. The metastases missed by PET were small (<9 mm). However, additional lesions were detected that were not seen by CT. Lucas et al. (43) also reported, in soft tissue sarcomas, metastatic spread outside the lungs, which was not seen by CT or MRI.

In summary, HRCT is the recommended modality for the detection of pulmonary metastases, particularly for <1 cm lesions; however, PET may add further information on whether these are malignant and may detect extrapulmonary metastases. Because benign pulmonary nodules are relatively common, particularly with newer helical CT scanners, not all lesions seen in the lungs in the context of primary osseous tumors are malignant. In the clinical situation where no previous investigations are available to determine the appearance or growth of lung nodules, PET can provide complementary information regarding the likelihood of malignancy. Those nodules that have intense FDG uptake are highly likely to represent metastases. Less intense FDG uptake should also be considered suspicious if the size of the nodule in question is less than twice the reconstructed spatial resolution of the PET scanner being used, because partial-volume effects significantly degrade count recovery for small lesions (44). For most modern PET scanners, this would

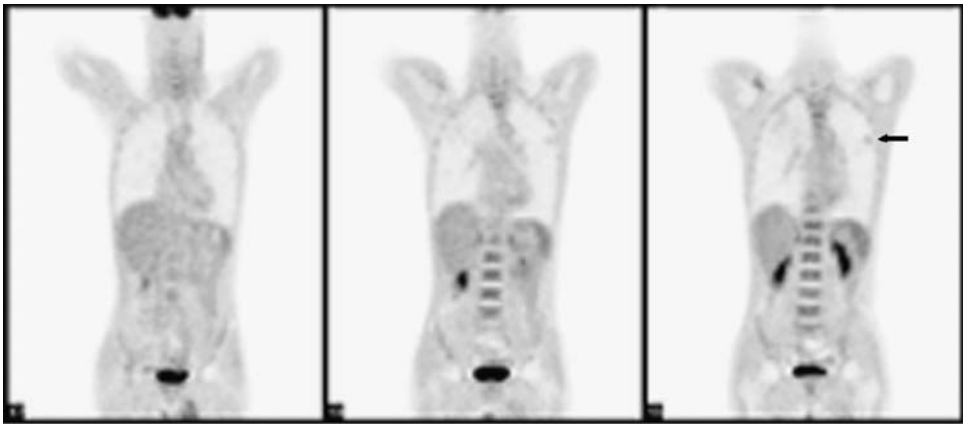

Figure 15.5. Pulmonary metastases. This patient with multifocal local recurrence related to osteosarcoma of the right lower leg (not shown) had multiple new lung nodules on CT scanning. Only the largest of these, a 9-mm left upper lobe lesion was clearly abnormal on FDG-PET (right coronal plane image). Nevertheless, the presence of metabolic abnormality in any nodules that are sufficiently large to be relatively unaffected by partial volume effects increases the likelihood that any other nonvisualized but smaller nodules are also malignant.

equate to lesions less than 10 mm in diameter. Respiratory excursion can also lead to partial volume effects, and one would generally expect somewhat lower FDG uptake in basal than apical lung nodules of comparable size due to greater respiratory blurring in the former. Finally, the avidity of the primary tumor is usually reflected in the intensity of uptake in metastatic sites. Accordingly, absence of FDG uptake in a lesion of 10 mm in the apex of the lung of a patient with an OS with a SUV_{max} of 25 is much more likely benign than malignant, whereas a lesion of the same size in the lung base of a patient with an ES with a SUV_{max} of 3.5 has a higher likelihood of malignancy on technical considerations alone. Of course, the radiologic features of the nodule, other clinical details, and the prevalence of benign lung nodules in the general population of the case in question also influence the likelihood of malignancy (Fig. 15.5).

Skeleton

The second most common area of metastatic disease is the skeleton, which occurs in 10% to 20% of patients with metastatic disease. Franzius et al. (45) looked at 70 patients with primary bone tumors (32 OS, 38 ES) for metastatic disease. The reference methods for imaging modalities were histopathologic analysis and conventional imaging with follow-up for 6 to 64 months. In 21 examinations, 54 osseous metastases were detected (5 OS, 49 ES). Fluorodeoxyglucose-PET had sensitivity, specificity, and accuracy of 90%, 96%, and 95%, respectively, compared to the radionuclide bone scan using technetium-99m (^{99m}Tc)-MDP [methylene diposphonate], which had 71%, 92%, and 88%, respectively. Interestingly, when the OS and ES were compared, the performance of PET relative to bone scanning differed. For ES, the

sensitivity, specificity, and accuracy of PET were 100%, 96%, and 97%, respectively, compared to bone scintigraphy of 68%, 87%, and 82%, respectively. However, none of the five OS osseous metastases were detected by FDG but were true positive on the bone scan. In a more recent publication by the same group, the authors reported 100% detection by FDG-PET in six sites of bony metastatic disease from OS (46). These differences may relate to the contrast resolution of the respective modalities. Very high osteoblastic activity in metastatic OS sites may improve lesion sensitivity even though the spatial resolution of planar and SPECT bone scanning is less than that of PET. Conversely, improvements in PET instrumentation including improved scanner resolution and better attenuation correction methods could also improve lesion sensitivity.

Daldrup-Link et al. (47) compared FDG-PET, bone scintigraphy, and whole-body MRI for detection of bone metastases from multiple types of malignancies. They looked at 39 children and young adults with various metastases including 20 patients with ES and three with OS. Of 51 bone metastases, the overall sensitivity for FDG-PET, whole-body MRI, and bone scintigraphy were 90%, 82%, and 71%, respectively. False-negative sites were different for the three modalities. In one patient with osteogenic sarcoma, a single metastasis was diagnosed with bone scintigraphy and MRI but was negative on FDG-PET. Most false-negative findings for PET were in the skull; for MRI in flat and small bones, the skull, carpal bones, and radius; and for bone scintigraphy in the spine. The number of skeletal metastases was inversely related to lesion size. Large lesions >5 cm were correctly diagnosed with FDG-PET and MRI in 100% of patients, but skeletal scintigraphy had a sensitivity of 93%. Sensitivity for smaller lesions of 1 to 5 cm for FDG-PET was 86%, MRI 79%, and skeletal scintigraphy 62%. For bone metastases <1 cm, FDG-PET showed a sensitivity of 86%, MRI 57%, and skeletal scintigraphy 57%. More false positives, however, were found with PET; they were, in this series, a simple bone cyst, an enchondroma, and an osteoma. The latter two were diagnosed with plain radiography. Increased sensitivities for detection of lesions were found by combining the modalities: for skeletal scintigraphy and MRI, 90%; for skeletal scintigraphy and FDG-PET, 96%; and for MRI and FDG-PET, 96%. Thus the sensitivities of skeletal scintigraphy and MRI alone were significantly increased either in combination with each other or with PET. But the sensitivity of PET was not increased significantly by combining with one of the other modalities. In clinical practice, as opposed to technical validation studies, PET should always be interpreted in the clinical context and with careful correlation of all the imaging results available in a given patient. The choice and order in which imaging studies are performed will also likely be determined by a multitude of factors including cost, convenience, and availability. Although bone scanning is relatively inexpensive and widely available, it is probably worthwhile in most cases of OS, but its role in ES and other sarcomas must be questioned if PET is available.

In the future there may be a role for ^{18}F-PET scans. Initial evaluation indicates a high detection rate for skeletal metastases. Accordingly, this

may enhance the sensitivity for metastases in OS compared to FDG-PET by virtue of higher lesion avidity and compared to bone scintigraphy by virtue of superior spatial resolution (13).

Other Secondary Sites

Metastases to other areas, for example, lymph nodes, brain, and soft tissue, are uncommon but can be detected by PET. There are no data comparing conventional radiology techniques with PET for this role. The ability of PET, however, to screen the whole body is a significant advantage (13,41,43).

Assessment of Response to Treatment

Response to preoperative adjuvant chemotherapy has been shown to be the most important prognostic factor in the management of OS and ES, as the degree of tumor necrosis from the therapy is highly correlated with disease-free survival after therapy (8,21,22). Due to the surgical and prognostic implications relating to an adequate response to neoadjuvant therapy, a noninvasive marker for assessing histologic response would be very clinically useful. Tumor necrosis can exist in the primary tumor and is itself a manifestation of large or aggressive tumors. It can be difficult to know on the basis of a small pretreatment biopsy the proportion of viable and nonviable tumor and therefore compare relative change in this parameter when confronted by a large excisional specimen posttreatment. Evaluation of early response to chemotherapy in primary bone tumors after 3 to 6 weeks of therapy may be highly predictive of tumor necrosis; whether PET is valid for this purpose requires further study. In this way, noninvasive assessment of chemotherapy response by PET may significantly alter patient management (Figs. 15.2 and 15.3). For instance, limb-sparing surgery is more likely to be considered if there is a favorable response to chemotherapy. There may be an alteration in surgical approach. Also if there is an unfavorable response several investigators recommend a change in chemotherapeutic regimen. The earlier that this can be detected, the earlier the change can be made (4,5,8,13).

Radiologic methods such as radiography, CT, and MRI are poorly suited for discriminating adequately between responding and nonresponding osseous tumors. The tumors frequently do not change in size, or there may be some minor change in the soft tissue mass around the osseous component. The response of the tumor detected by using these conventional methods does not reflect the quantity of residual viable tumor. New techniques using dynamic contrast-enhanced MRI have been shown to improve the differentiation of viable sarcoma tissue from tumor necrosis as an early indicator of recurrence. This technique is promising and needs further evaluation (18,48,49).

Functional nuclear medicine biological methods such as thallium 201 (^{201}Tl), ^{99m}Tc sestamibi, and FDG-PET have been shown to be effective response markers for chemotherapy assessment in primary bone tumors (17). ^{201}TI and ^{99m}Tc sestamibi have been used to determine

grade and response to chemotherapy. A negative ^{201}Tl or ^{99m}Tc sestamibi scan after therapy reflected a grade III to IV response with >90% necrosis of tumor cells. Kostakoglu et al. (50) reported for ^{201}Tl a sensitivity of 100%, specificity of 87.5%, and accuracy of 96.5% compared to sensitivities of 95%, 50%, and 82.7%, respectively, for CT, MRI, and angiography in bone and soft tissue sarcomas. However, FDG-PET with its uptake quantifiable by using SUV or T/BG ratios adds further information and is recommended if available.

Jones et al. (51) were one of the first groups to report the impact of FDG-PET in the monitoring of treatment in patients with musculoskeletal sarcoma, 3 of whom had OS. The authors observed a 25% to 50% reduction of the peak and average SUV, 1 to 3 weeks after chemotherapy was instituted; this correlated with >90% tumor cell necrosis. They also reported that there was increased FDG uptake seen in granulation tissue and in the pseudofibrous capsule in treated cancers. This indicates that there is FDG uptake in both the viable tumor and some benign reactive tissues (Fig. 15.2C). This has the potential to overestimate the presence of OS. Other groups have reported changes in response to treatment in a significant number of patients with primary bone tumors by using PET and showed good correlation with histopathologic changes after treatment (Table 15.2) (41, 52, 53).

Franzius et al. (52) reported good correlation in 17 patients between T/NT ratios and primary bone tumors (11 OS, 6 ES). The mean T/NT was 5.2 (range 2.2–13.6) for all 17 patients with posttherapy values of 2.3 (0.9–11.9). For OS pretherapy T/NT was 5.5 (2.3–13.6) and posttherapy 2.8 (0.9–11.9); for ES the pretherapy was 5.3 (2.2–11.9) and posttherapy 1.4 (1.0–1.9). There was good correlation with tumor necrosis on histopathology in 15 of 17 overall, in 9 of 11 patients with OS, and in all 6 of the patients with ES. The authors found that a threshold of a 30% decrease in the ratio represented good responders (<10% viable tumor cells) and could distinguish these patients from poor responders in all cases.

Hawkins et al. (53) looked at SUV values of FDG-PET uptake in 14 OS and 14 ES patients. They used SUV_{max} values in tumors pre-(SUV1) and post-(SUV2) chemotherapy. They demonstrated that a reduction in tumor FDG uptake, measured by $SUV2_{max}$ and the ratio of SUV2/SUV1, correlated with chemotherapy response as quantified by percent necrosis after surgical resection. In OS SUV1 was 8.2 (2.5–24.1) and decreased to SUV2 of 3.3 (1.6–12.8) after chemotherapy; SUV2 was particularly accurate in identifying OS patients with unfavorable response. In the ES group, the SUV1 was 5.3 (range 2.3–11.8) and decreased to SUV2 of 1.5 (0–2.4) posttherapy. The mean percent necrosis of the OS group was lower than the ES group; only 28% of OS tumors responded adequately with a mean percent necrosis of >90%. However, the authors report that both the SUV2 and SUV2/SUV1 ratio are imperfect at distinguishing favorable from unfavorable responses. Using a cutoff point of <2 for SUV2 to predict favorable response was incorrect in 16% and using a cutoff point of <0.5 for SUV2/SUV1 for a favorable response was incorrect in 27% of patients. The most likely

Table 15.2. Changes in response to treatment in patients with primary bone tumors

Study	Pathology	Pretherapy SUV1, T/NT1, T/BG1,	Posttherapy SUV2, T/NT2, T/BG2	Response	Correlation with necrosis
Franzius et al. (52)	17 BS	T/NT mean 5.2 (2.2–13.6)	T/NT mean 2.3 (0.9–11.9)	15/17 good	Yes
	11 OS	T/NT 5.5 (2.3–13.6)	T/NT 2.8 (0.9–11.9)	9/11 good	Yes
	6 ES	T/NT 5.3 (2.2–11.9)	T/NT 1.4 (1.0–1.9)	6/6 good	Yes
Hawkins et al. (53)	18 OS	SUV_{mean} 8.2 (2.5–24.1)	SUV_{mean} 3.3 (1.6–12.8)	Yes	Mean 66% (0–98%)
	15 ES	SUV 5.3 (2.3–11.8)	SUV_{mean} (0–2.4)	Yes	Mean 98% (90–100%)
			OS SUV2/SUV1 0.55 (0.12–1.1) ES SUV2/SUV1 0.35 (0.16–0.73)		
Schulte et al. (41)	27 OS	T/BG 10.3 (3.3–33.2)			
	Responder	T/BG 10.34 (3.89–33.2)	T/BG 2.27 (0.32–17.5)	Good	Yes
	Nonresponder	T/BG 9.64 (3.26–22.2)	T/BG 6.37 (2.24–20.33)	Poor	Yes
Jones et al. (51)	9 ST and BS	SUV_{max} 5.8 (2.0–12.0) 6/9 high grade	SUV_{max} 3.3 (2.3–4.3) 2/9	3 OS Yes	>90% Yes
		SUV_{mean} 3.6 (1.7–6.1)	SUV_{mean} 2.1 (1.8–2.3) 2/9		

BS = Bone sarcoma; ES = Ewing sarcoma; OS = steogenic sarcoma; ST = Soft Tissue Sarcoma; SUVm = SUVmean; T/BG = Tumor/Background; T/NT = Tumor/Nontumor.

explanation was due to increased FDG uptake in inflammatory infiltrates or reactive fibrosis within the tumor as a response to chemotherapy. Other reasons are that the histopathologic evaluation averages the percentage of necrosis across the entire resected tumor specimen, whereas the SUV technique is based on the maximum value within the tumor. Stated another way, a specimen that is extensively necrotic but with isolated foci of viable tumor would be classified as favorable, but the maximum SUV may remain elevated reflecting the focal viable tumor. A method similar to that proposed by Larson et al. (54)

that integrates the extent and intensity of metabolic activity may be useful in such situations. The methodology to define the volume of abnormal voxels—whether single or multiple voxels should be used—for determination of the degree of SUV abnormality remains to be established (18).

Schulte et al. (41), studying 27 patients with OS using T/BG ratios, found a reduction in T/BG of >40% represented responders to chemotherapy with an accuracy of 92.6%. The T/BG before therapy in all patients ranged from 3.3 to 33.2 (median 10.3). In the responder group, the pretherapy T/BG was 10.34 (3.89–33.2) and in nonresponders 9.64 (3.26–22.2). The posttherapy T/BG was for responders 2.27 (0.32–17.5) and nonresponders 6.37 (2.24–20.33). The posttherapeutic values differed significantly between the responders and nonresponders. The extent of T/BG reduction, however, did not precisely predict the quantitative amount of tumor necrosis. They did not report any false-positive cases where they classified a responder as a nonresponder due to benign reactive uptake as described by Jones et al. (51).

Serial assessments to monitor chemotherapeutic response were also discussed by Nair et al. (55). They looked at 16 patients with OS. The percentage change in tumor to background ratio (T/BR) did not predict a 90% or higher rate of tumor necrosis. Visual assessment and T/BR values, however, were predictive in 15 of 16 patients.

Further evaluation of the optimal quantitative method to assess response should be undertaken, but the present data indicate that FDG-PET is a relatively accurate indicator of tumor response to neoadjuvant therapy.

Local Tumor Recurrence

The ability to detect residual viable tumor after therapy and to detect local recurrence of tumor as early as possible is vital for improvement in survival. It is also one of the most difficult areas of management. Conventional imaging has significant limitations because of changes in normal anatomy, distortion of tissue planes, and lack of distinction between tumor and postoperative tissue, and image artifacts from metallic limb prostheses. Differentiation from fibrosis, posttherapeutic changes, and inflammatory tissue changes can be extremely difficult. Magnetic resonance imaging with gadolinium enhancement may also show increased enhancement in immature scar tissue and nonmalignant reactive tissue (56). Most of the comparisons of MRI and FDG-PET for the assessment of residual viable tumor and local recurrence relate to soft tissue sarcomas, presumably due to the inherent difficulties in evaluating periprosthetic sites. Garcia et al. (57) reported FDG was helpful in differentiating active musculoskeletal sarcomas from posttreatment changes in 48 patients. There were 18 patients with OS. The diagnosis was confirmed by histology, and the sensitivity and specificity were 98% and 90%, respectively. Similar results were found by el-Zeftawy et al. (58) in 20 patients with both bone and soft tissue tumors. The authors' conclusion was that FDG added important infor-

mation to CT and MRI to help differentiate postoperative change from local recurrence (Fig. 15.6). Franzius et al. (46) also reported detection of local recurrence in 6 patients with OS but had 1 false-negative study. In the same group of patients, the MRI detected all 6 recurrences, but there were 2 false-positive studies. In another group, Lucas et al. (43) found that MRI had a higher sensitivity of 88.2% compared to PET of 73.7% for the detection of local recurrence of soft tissue sarcomas after amputation. There are, however, significant difficulties with CT and MRI in patients with implantation of metallic prostheses (59). Hains et al. (60) described the limitations of FDG-PET in detecting local recurrence in amputation stumps. In their study, focal areas of FDG were seen in known pressure areas and skin breakdown for up to 18 months after surgery. However, in the absence of localized clinical changes in the stump, any uptake may represent recurrence and should be biopsied (Fig. 15.7). The co-registration of PET with CT or MRI should help significantly in these cases.

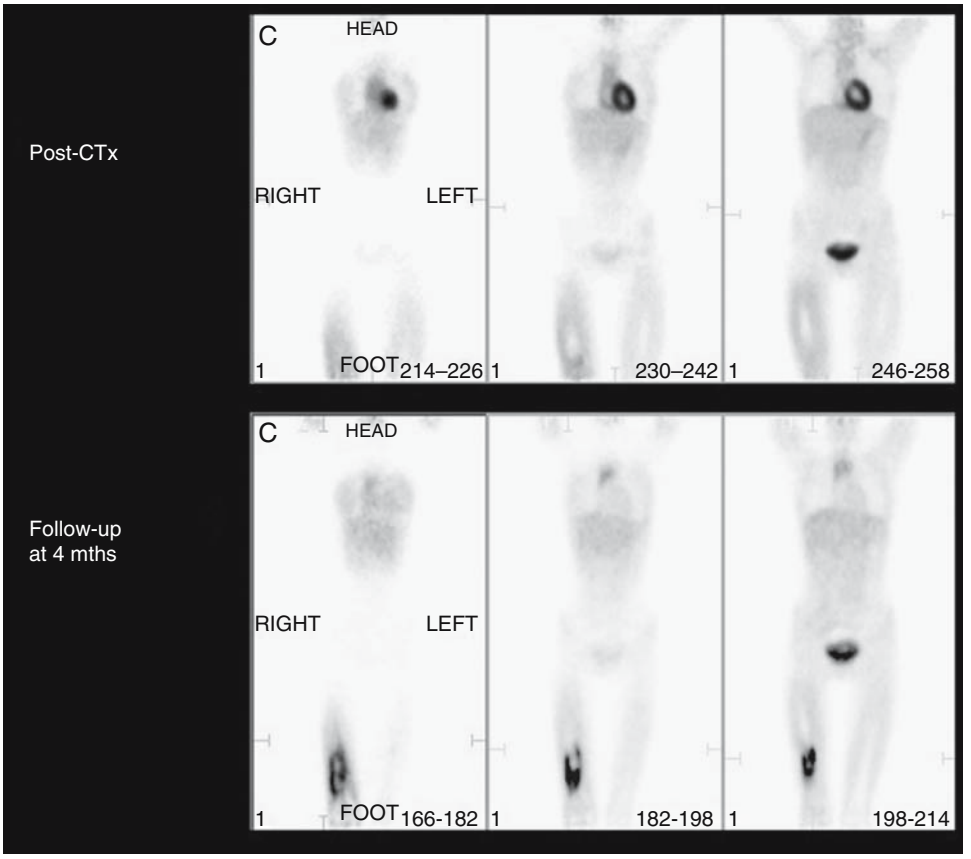

Figure 15.6. Recurrence. This patient had undergone chemotherapy for a distal right femoral Ewing sarcoma. The posttherapy PET scan demonstrated a very good but partial metabolic response with mildly increased activity inferomedially in the femur. A follow-up scan (below) performed 4 months later demonstrates extensive local recurrence. Note normal thymic uptake in an adolescent.

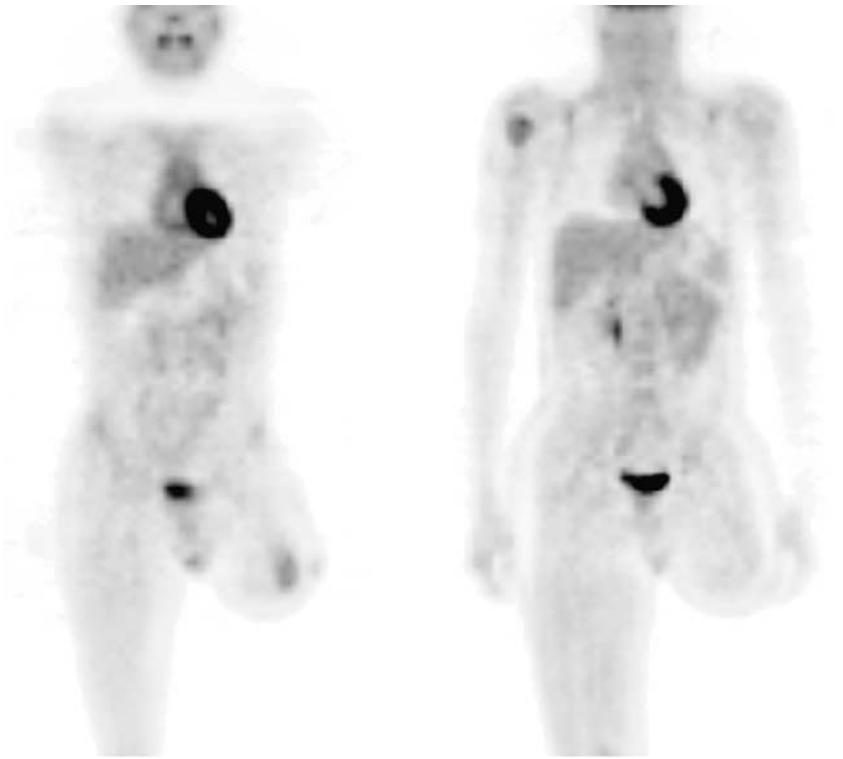

Figure 15.7. Recurrence of osteogenic sarcoma in amputation stump and development of skeletal metastases. This patient had a primary osteogenic sarcoma (OS) of the left femur removed 2 years previously. The PET study shows recurrence in the amputation stump and a metastatic deposit in the proximal right humerus. The patient developed multiple skeletal metastases over the following 6 months and died.

Other PET Radiopharmaceutical Agents

Fluorine-18 Fluoride

Unchelated fluorine-18 fluoride (^{18}F) was introduced as a bone imaging agent in 1962 (61). It became the standard for bone scanning until the introduction of ^{99m}Tc–labeled diphosphonates. It has a similar mechanism of uptake to the latter, depending on local blood flow for tracer delivery, diffusion through extracellular fluid to the bone mineral interface, and adsorption to the hydroxyapatite crystal to form fluoroapatite (62). Therefore, uptake reflects osteoblastic activity.

Inevitable comparisons have been made with ^{99m}Tc diphosphonate bone scans. One cited advantage of ^{18}F is superior pharmacokinetics. ^{18}F has a higher extraction rate and faster blood clearance, allowing imaging to commence as early as 1 hour after intravenous administration (63). Other advantages arise in combination with current generation PET or PET-CT scanners, allowing dynamic quantitation and superior spatial and contrast resolution. One main drawback is the

higher cost of ^{18}F compared to the more widely available diphosphonate radiopharmaceuticals. However, as FDG production increases, ^{18}F fluoride production as a by-product could become more efficient and decrease radiotracer costs.

To date there has been little published experience with ^{18}F-PET in primary bone tumors and even less for the pediatric population. One early series was from Hoh et al. (63), who reported their experience in 19 adult patients with a mix of benign and malignant bone pathologies. Using visual and a semiquantitative assessment (uptake ratio of lesion-to-contralateral bone), it was not possible to differentiate benign from malignant lesions. Of interest, there were 4 patients with OS in the group. The three patients who had no prior treatment had primary tumors with the highest uptake ratios in the study. The other patient's scan followed systemic therapy; the uptake here was lower than the other three, suggesting a potential role for ^{18}F-PET in therapeutic monitoring. Three of these 4 patients had multiple scan lesions, indicating that metastases were also visualized, both skeletal and pulmonary. One patient was specifically mentioned with uptake in multiple pulmonary nodules.

Going further than the above study, would formal dynamic ^{18}F-PET quantitation with blood sampling improve either the differentiation between benign and malignant lesions or be incorporated into therapeutic monitoring of primary bone tumors? As yet no studies have addressed this question. However, we can look at the experience with ^{99m}Tc diphosphonates where there is a similar mechanism of uptake. Just as reactive bone formation or turnover often accounts for more bone tracer localization than uptake by viable tumor, it is predicted that ^{18}F-PET would be similarly unsuccessful (64).

There are more studies of ^{18}F-PET for metastatic surveys. Although these have again been mostly adult patients with unselected cancers, many of the observations should be relevant here. Conventional bone scans have a lower resolution, and almost all are planar images, with single photon emission computed tomography (SPECT) limited to a localized region of the body. The higher resolution and whole-body tomography intrinsic to ^{18}F-PET predicts superior diagnostic performance. Schirrmeister et al. (65–67) found this to be the case in series of patients with breast, lung, prostate, and thyroid cancer. Superior resolution in the spine allowed more specific diagnosis over conventional planar bone scans (67). This observation was taken a step further with the more recent study of ^{18}F-PET-CT vs. ^{18}F-PET from Even-Sapir et al. (68). One would expect that the improved lesion localization from PET/CT would improve diagnostic accuracy, and this was the case. Their study population ranged in age from 15 to 81 years old. There were three cases of ES, one chondrosarcoma, and one giant cell tumor. In a patient-based analysis for the detection of metastatic disease, ^{18}F-PET-CT was superior to ^{18}F-PET alone in sensitivity (100% vs. 88%, $p < .05$) and specificity (88% vs. 56%, not significant). Therefore, this is the most promising area for ^{18}F-PET; more studies of specific tumor types, including pediatric primary bone tumors, are awaited. The feasibility of acquiring ^{18}F-PET and ^{18}F-FDG-

PET scans at one clinic attendance is another interesting area for study.

^{18}F-α-Methyltyrosine

After promising initial studies with iodine-123–labeled methyltyrosine (69), fluorine-18 α-methyltyrosine (^{18}FMT) was developed for PET imaging (70). It is a tracer for the increased amino acid utilization by tumors, as is carbon-11 (^{11}C) methionine (see below), but it has a significant advantage by virtue of its tumor-specific transport. Watanabe et al. (71) reported a comparison between ^{18}FMT and ^{18}F-FDG in baseline pretreatment musculoskeletal tumors. The study group comprised 75 patients with benign and malignant tumors and included three patients (ages 14 to 34 years) with OS, a 12-year-old patient with ES, and adult patients with chondrosarcoma and giant cell tumor. All malignant bone tumors showed ^{18}FMT uptake. Of note, there was also uptake within a pulmonary metastasis from OS. There was higher uptake in malignant lesions than benign, and there was good correlation with ^{18}F-FDG uptake. Using ^{18}FMT mean SUV cutoff of 1.2 to differentiate benign vs. malignant lesions, the diagnostic accuracy was 81.3%, which was higher than the respective analysis for ^{18}F-FDG. Thirteen of 18 lesions that were false positive on ^{18}F-FDG were found to have an ^{18}FMT mean SUV lower than the cutoff and would have been correctly classified as benign. However, ^{18}FMT was found to be inferior for grading of malignancy. It was suggested that the lower absolute values and ranges of its mean SUV were responsible. In summary, another promising alternative to ^{18}F-FDG and more studies are awaited.

Fluorine-18 fluoro-3′-deoxy-3′-L-fluorothymidine

Fluorine-18 fluoro-3′-deoxy-3′-L-fluorothymidine (FLT) has been developed as a proliferative tracer to provide a noninvasive staging tool and to measure response to anticancer therapy (72). Proliferating cells synthesize DNA during the S phase of the cell cycle. FLT is a pyrimidine analogue and uses the salvage pathway of DNA synthesis for imaging proliferation. The ability to image cell proliferation may offer the possibility to differentiate between benign and malignant disease. FLT is taken up by the cell via passive diffusion and facilitated transport by Na^+-dependent carriers. FLT is then phosphorylated by thymidine kinase (TK) into FLT monophosphate, after which it is trapped in the cell. Preliminary comparisons with FDG show that FLT can visualize malignant cancers but at a lower sensitivity than FDG. Some tumors metabolically rely on the de novo synthesis of DNA precursors, resulting in little or no uptake of thymidine and FLT. As a proliferative marker, because FLT is phosphorylated by TK, which has high activity in the S phase of cell synthesis. There are higher concentrations of FLT in malignant cells compared to normal cells. There have been several reports of strong correlation of FLT with other proliferative markers (Ki-67 index). As tumor mass heterogeneity is visualized, there is the potential for determining optimal biopsy sites (Fig. 15.8).

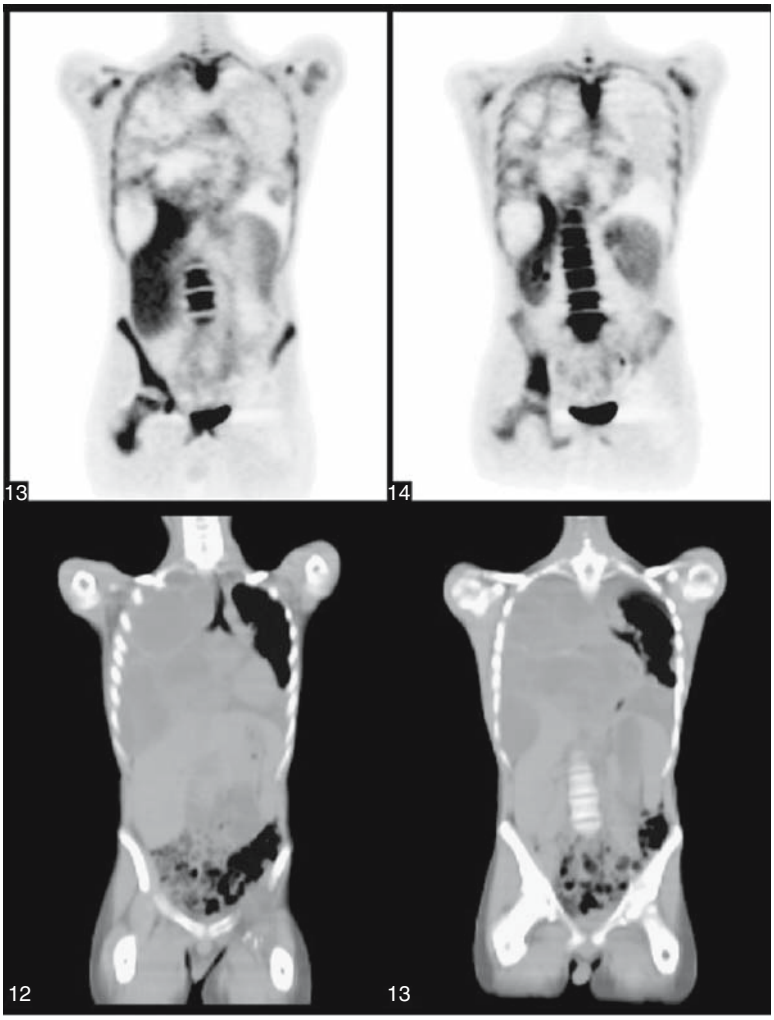

Figure 15.8. Fluorine-18 fluoro-3′-deoxy-3′-L-fluorothymidine (FLT) in sarcoma. Following radiotherapy for a synovial sarcoma of the left hip, this adolescent boy developed progressive right lung metastases and bilateral pleural effusions. ^{18}F-FLT-PET scanning demonstrates heterogeneous uptake in the opacified right hemithorax with very low uptake in the bilateral basal pleural effusions and in areas of necrotic tumor but relatively high uptake at the periphery of solid tumoral deposits indicating active proliferation. Note the high uptake in the bone marrow with the exception of the irradiated left hip, where there is no uptake consistent with local marrow ablation. High uptake in the kidneys and liver reflect normal excretion but limit detection of metastatic disease in these organs. The spleen is also visualized, displaced inferiorly and medially by the left basal pleural effusion. In our experience, the spleen is not normally visualized in adults except in cases of extramedullary hematopoiesis or malignant infiltration.

In the initial data on assessment of response to anticancer therapy, FLT uptake has been shown to decrease after some therapy but may increase after other types. This would most likely be due to the various metabolic actions of the different chemotherapeutic agents. Preliminary studies using FLT have been reported in various tumors, including soft tissue sarcoma. Cobben et al. (73) found correlations among SUV and T/NT and mitotic score, Ki-67, and the French and Japanese grading systems. Visualization of the tumors was good, and FLT was able to differentiate between low- and high-grade tumors. However, no differentiation could be made between benign and low-grade tumors. This agent appears promising and potentially may be useful in primary bone tumors. However, further research is needed to clarify the value of FLT in cancer management. High uptake of FLT in normal proliferating marrow may limit sensitivity for detection of bone metastases and for evaluating the extent of marrow spread in marrow-containing regions of the skeleton. This poses a potential limitation, particularly in pediatric patients, because of more extensive appendicular marrow than seen in adults (72,73).

Carbon-11–Based Tracers

Carbon-11–labeled methionine (^{11}C-Met) was developed as a tracer for the increased amino acid metabolism in tumors. There are few studies on extracranial tumors, in part because of its participation in too many metabolic pathways to allow kinetic modeling (74). Of the published studies of ^{11}C-Met, only a few relate to primary bone tumors. Inoue et al. (75) studied 24 adult patients with clinically suspected recurrent or residual tumors, using ^{11}C-Met and ^{18}F-FDG-PET. Their group included one case of proven recurrent pelvic ES where ^{11}C-Met was false negative but was detected by ^{18}F-FDG. Both PET agents were false negative in one case of recurrent pelvic chondrosarcoma, but both were true positive in two cases of recurrent giant cell tumor. Therefore, the early report card for ^{11}C-Met is mixed; it is not clearly superior to ^{18}F-FDG.

Methyl-C-11 choline (^{11}C-choline) takes advantage of increased tumor requirements for choline, which is phosphorylated, integrated within lecithin, and finally becomes a component of the phospholipid cell membrane (76). After injection, tumor uptake equilibrates at 5 minutes, allowing earlier image acquisition than is the case with ^{18}F-FDG. Another potential advantage of ^{11}C-choline is that it does not accumulate in the bladder compared with the usual urinary excretion of FDG, a consideration when evaluating pelvic lesions. The application to bone and soft tissue tumors has been published in two articles from the Gunma University group comparing ^{11}C-choline and ^{18}F-FDG-PET scans, with what appears to be some overlap of both study samples (77,78). Yanagawa et al. (77) reported only patients at pretreatment baseline. Their first group included 5 ranging in age from 11 to 20 years with OS. Zhang et al. (78) appear to have included some patients undergoing therapy, but the 2 scans were acquired within 2 weeks of each other with no change in therapy. This second group

included 2 older patients with OS and 2 patients (17 and 24 years old) with ES. Both studies included other benign and malignant tumors. All malignant tumors showed ^{11}C-choline uptake, and their mean tumor SUV was higher than benign tumors. ^{11}C-choline uptake showed good correlation with ^{18}F-FDG uptake. However, significant ^{11}C-choline uptake was also seen in some benign tumors in both study groups, viz. giant cell tumor, desmoid tumor, fibroma, neurofibroma, inflammatory granulation tissue, and pigmented villonodular synovitis. When analyzing the ability of ^{11}C-choline to differentiate benign from malignant lesions, both groups used different mean SUV cutoff values—2.7 for a diagnostic accuracy of 90.9% (77) and 2.59 for a diagnostic accuracy of 75.6% (78). The differing result was attributed to the inclusion of more benign lesions in the latter analysis. However, when compared with the respective ^{18}F-FDG mean SUV cutoffs in a receiver operating characteristic analysis, both studies found that ^{11}C-choline had a higher diagnostic accuracy. In summary, if ^{11}C-choline becomes more widely available, it may be a useful alternative to ^{18}F-FDG. It may have a problem-solving role in tumors located near the urinary bladder and possibly in cases where there is uncertainty about benign vs. malignant pathology. Newer fluorinated choline analogues (79) are of interest and may be more practical for clinical use due to a longer physical half-life.

Technical Issues

In oncology, radiation dosimetry from diagnostic imaging tests is a more important consideration for pediatric than for adult patients because of a generally higher survival rate and a longer potential period of life to manifest adverse consequences of radiation exposure in children, as well as issues of differential susceptibility to the effects of radiation. Accordingly, minimization of radiation dose is an important consideration in the pediatric population. Although PET utilizes isotopes with relatively high gamma photon energy (511 keV) and with a particulate (positron) emission, the short half-life of ^{18}F and other PET tracers offer significant advantages compared to other competing tracers used for oncologic imaging, such as ^{201}Tl and ^{67}Ga. The high sensitivity of PET generally allows administration of relatively small doses of radiotracer to pediatric patients, particularly if three-dimensional (3D) imaging is performed. Although 3D body imaging using PET can be degraded by a significant scatter fraction in adults, this is seldom an issue in children. We believe that 3D acquisition is preferable, if available, for imaging children less than 60 kg in weight. Sensitive PET detectors like thick sodium iodide crystals used in the C-PET (Philips [Milpitas, California]) and various modified gamma cameras have particular appeal for pediatric patients, although their performance is somewhat compromised in larger patients compared to modern bismuth germanate oxide (BGO) and lutetium oxyorthosilicate (LSO) based PET scanners. The incremental benefits of PET-CT in terms of diagnostic confidence and localization ability also need to be balanced with the additional radiation burden of adding a helical CT

acquisition to the PET procedure. Low-dose CT acquisitions yield very good quality CT for correlation and attenuation correction purposes in our opinion.

Conclusion

Positron emission tomography imaging with ^{18}F-FDG has been shown to significantly impact patient management in primary bone tumors by improving the initial diagnosis with more accurate staging, determining whether there is metastatic disease, providing an accurate indicator of response to treatment, detecting early recurrence, and finally by providing an accurate indicator for patient prognosis. The most efficient method is a combination of PET with other anatomic imaging modalities, that is, CT and MRI. Several other PET radiopharmaceuticals also show great promise. For the medical imaging evaluation of primary bone tumors in our young patients, the already essential role of PET is likely to expand further with newer developments and applications. Recognition that PET, as a molecular imaging technique, is more about lesion characterization than lesion counting will enable realistic expectations of how and when to use PET in the diagnostic process. With such a disparate range of diseases, outcomes, and therapeutic options, we believe that prognostic stratification may well be the most important function provided by PET.

References

1. Phan A, Patel S. Advances in neoadjuvant chemotherapy in soft tissue sarcomas. Curr Treat Options Oncol 2003;4(6):433–439.
2. Bacci G, Lari S. Current treatment of high grade osteosarcoma of the extremity: review. J Chemother 2001;13(3):235–243.
3. Ballo MT, Zagars GK. Radiation therapy for soft tissue sarcoma. Surg Oncol Clin North Am 2003;12:449–467.
4. Meyers PA, Gorlick R. Osteosarcoma. Pediatr Clin North Am 1997;4: 973–989.
5. Grier HE. The Ewing family of tumors. Pediatr Clin North Am 1997;4: 991–1104.
6. Mirra JM. Osteosarcoma: intramedullary variants. In: Mirra JM, ed. Bone Tumors. Philadelphia: Lea & Febiger, 1989:249–389.
7. Mirra JM, Picci P. Ewing's sarcoma. In: Mirra JM, ed. Bone Tumors. Philadelphia: Lea & Febiger, 1989:1087–1117.
8. Arndt CAS, Crist WM. Common musculoskeletal tumors of childhood and adolescence. N Engl J Med 1999;341(5):342–352.
9. Rodriguez-Galindo C, Spunt SL, Pappo AS. Treatment of Ewing sarcoma family of tumors: current status and outlook for the future. Med Pediatr Oncol 2003;40:276–287.
10. Bruland OS, Pihl A. On the current management of osteosarcoma: a critical evaluation and a proposal for a modified treatment strategy. Eur J Cancer 1997;33:1725–1731.
11. Raymond AK, Chawla SP, Carrasco CH, et al. Osteosarcoma chemotherapy effect: a prognostic factor. Semin Diagn Pathol 1987;4:212–236.

12. Eary JF, Conrad EU, Bruckner JD, et al. Quantitative [F-18] fluorodeoxyglucose positron emission tomography in pretreatment and grading of sarcoma. Clin Cancer Res 1998;4:1215–1220.
13. Brenner W, Bohuslavizki KH, Eary JF. PET imaging of osteosarcoma. J Nucl Med 2003;44(6):930–942.
14. Messa C, Landoni C, Pozzato C, Fazio F. Is there a role for FDG PET in the diagnosis of musculoskeletal neoplasms? J Nucl Med 2000;41(10): 1702–1703.
15. Oliveira AM, Nascimento AG. Grading in soft tissue tumors: principles and problems. Skeletal Radiol 2001;30:543–559.
16. Hicks RJ. Nuclear medicine techniques provide unique physiologic characterization of suspected and known soft tissue and bone sarcomas. Acta Orthop Scand 1997;273(suppl):25–36.
17. Hicks RJ. Functional imaging techniques for evaluation of sarcomas. Cancer Imaging 2005;5:58–65.
18. Hicks RJ, Toner G, Choong PFM. Clinical applications of molecular imaging in sarcoma evaluation. Cancer Imaging 2005;5:66–72.
19. Miller SL, Hoffer FA. Malignant and benign bone tumors. Radiol Clin North Am 2001;39:673.
20. Siegel MJ. Magnetic resonance imaging of musculoskeletal soft tissue masses. Radiol Clin North Am 2001;39:701–720.
21. Rosen G, Caparros B, Groshen S. Primary osteogenic sarcoma of the femur: a model for the use of preoperative chemotherapy in high risk malignant tumours. Cancer Invest 1984;2:181–192.
22. Picci P, Rougraff BT, Bacci G, et al. Prognostic significance of histopathologic response to chemotherapy in non metastatic Ewing sarcoma of the extremity. J Clin Oncol 1993;11:1763–1769.
23. San-Julian M, Dolz R, Garcia-Barrecheguren E, et al. Limb salvage in bone sarcomas in patients younger than age 10. J Pediatr Orthop 2003;23: 753–762.
24. Wodajo FM, Bickels J, Wittig J, Malawer M. Complex reconstruction in the management of extremity sarcomas. Curr Opinion Oncol 2003;15:304–312.
25. Picci P, Sangiorgi L, Rougraff BT, et al. Relationship of chemotherapy-induced necrosis and surgical margins to local recurrence in osteosarcoma. J Clin Oncol 1994;12:2699–2705.
26. Glasser D, Lane J, Huvos A, et al. Survival, prognosis and therapeutic response in osteogenic sarcoma: the Memorial Hospital experience. Cancer 1992;69:698–708.
27. Townsend DW, Beyer T, Blodgett TM. PET/CT scanners: a hardware approach to image fusion. Semin Nucl Med 2003;33:193–204.
28. Kern KA, Brunetti A, Norton JA, et al. Metabolic imaging of human extremity musculoskeletal tumors by PET. J Nucl Med 1988;29:181–186.
29. Adler LP, Blair HF, Makley JT, et al. Noninvasive grading of musculoskeletal tumors using PET. J Nucl Med 1991;32(8):1508–1512.
30. Hoh CK, Hawkins RA, Glaspy JA, et al. Cancer detection with whole-body PET using 2–[^{18}F]fluoro-2–deoxy-D-glucose. J Comput Assist Tomogr 1993;17:582–589.
31. Eary JF, O'Sullivan F, Powitan Y, et al. Sarcoma tumor FDG uptake measured by PET and patient outcome: a retrospective analysis. Eur J Nucl Med Mol Imaging 2002;29(9):1149–1154.
32. Folpe AL, Lyles RH, Sprouse JT, Conrad EU III, Eary JF. (F-18) fluorodeoxyglucose positron emission tomography as a predictor of pathologic grade and other prognostic variables in bone and soft tissue sarcoma. Clin Cancer Res 2000;6(4):1279–1287.

33. Schulte M, Brecht-Krauss D, Heymer B, et al. Grading of tumors and tumorlike lesions of bone: evaluation by FDG PET. J Nucl Med 2000; 41(10):1695–1701.
34. Feldman F, van Heertum R, Manos C. 18FDG PET scanning of benign and malignant musculoskeletal lesions. Skeletal Radiol 2003;32(4):201–208.
35. Dimitrakopoulou-Strauss A, Strauss LG, Heichel T, et al. The role of quantitative (18)F-FDG PET studies for the differentiation of malignant and benign bone lesions. J Nucl Med 2002;43(4):510–518.
36. Aoki J, Watanabe H, Shinozaki T, et al. FDG PET of primary benign and malignant bone tumors: standardized uptake value in 52 lesions. Radiology 2001;219(3):774–777.
37. Watanabe H, Shinozaki T, Yanagawa T, et al. Glucose metabolic analysis of musculoskeletal tumours using 18-fluorine-FDG PET as an aid to preoperative planning. J Bone Joint Surg [Br] 2000;82(5):760–767.
38. Kole AC, Nieweg OE, Hoekstra HJ, van Horn JR, Koops HS, Vaalburg W. Fluorine-18–fluorodeoxyglucose assessment of glucose metabolism in bone tumors. J Nucl Med 1998;39(5):810–815.
39. Franzius C, Bielack S, Flege S, Sciuk J, Jurgens H, Schober O. Prognostic significance of (18)F-FDG and (99m)Tc-methylene diphosphonate uptake in primary osteosarcoma. J Nucl Med 2002;43(8):1012–1017.
40. Jaramillo D, Laor T, Gebhardt MC. Pediatric musculoskeletal neoplasms: evaluation with MR imaging. MRI Clin North Am 1996;4(4):749–770.
41. Schulte M, Brecht-Krauss D, Werner M, et al. Evaluation of neoadjuvant therapy response of osteogenic sarcoma using FDG PET. J Nucl Med 1999;40(10):1637–1643.
42. Franzius C, Daldrup-Link HE, Sciuk J, et al. FDG-PET for detection of pulmonary metastases from malignant primary bone tumors: comparison with spiral CT. Ann Oncol 2001;12:479–486.
43. Lucas JD, O'Doherty MJ, Wong JC, et al. Evaluation of fluorodeoxyglucose positron emission tomography in the management of soft-tissue sarcomas. J Bone Joint Surg [Br] 1998;80:441–447.
44. Pitman AG, Hicks RJ, Binns DS, et al. Performance of sodium iodide based ^{18}F-fluorodeoxyglucose positron emission tomography in the characterisation of indeterminate pulmonary nodules or masses. Br J Radiol 2002;75:114–121.
45. Franzius C, Sciuk J, Daldrup-Link HE, Jurgens H, Schober O. FDG-PET for detection of osseous metastases from malignant primary bone tumours: comparison with bone scintigraphy. Eur J Nucl Med 2000;27(9):1305–1311.
46. Franzius C, Daldrup-Link HE, Wagner-Bohn A, et al. FDG-PET for detection of recurrences from malignant primary bone tumors: comparison with conventional imaging. Ann Oncol 2002;13:157–160.
47. Daldrup-Link HE, Franzius C, Link TM, et al. Whole-body MR imaging for detection of bone metastases in children and young adults: comparison with skeletal scintigraphy and FDG PET. AJR 2001;177(1):229–236.
48. Tacikowska M. Dynamic magnetic resonance imaging in soft tissue tumors—assessment of the diagnostic value of tumor enhancement rate indices. Med Sci Monitor 2002;8(4):MT53–MT57.
49. Negendank WG. MR spectroscopy of musculoskeletal soft-tissue tumors. MRI Clin North Am 1995;3:713–725.
50. Kostakoglu L, Panicek DM, Divgi CR, et al. Correlation of the findings of thallium-201 chloride scans with those of other imaging modalities and histology following therapy in patients with bone and soft tissue sarcomas [erratum in Eur J Nucl Med 1996;23(11):1558]. Eur J Nucl Med 1995;22(11): 1232–1237.

51. Jones DN, McCowage GB, Sostman HD, et al. Monitoring of neoadjuvant therapy response of soft-tissue and musculoskeletal sarcoma using fluorine-18–FDG PET. J Nucl Med 1996;37(9):1438–1444.
52. Franzius C, Sciuk J, Brinkschmidt C, Jurgens H, Schober O. Evaluation of chemotherapy response in primary bone tumors with F-18 FDG positron emission tomography compared with histologically assessed tumor necrosis. Clin Nucl Med 2000;25(11):874–881.
53. Hawkins DS, Rajendran JG, Conrad EU III, Bruckner JD, Eary JF. Evaluation of chemotherapy response in pediatric bone sarcomas by [F-18]-fluorodeoxy-D-glucose positron emission tomography [erratum appears in Cancer 2003;97(12):3130]. Cancer 2002;94(12):3277–3284.
54. Larson SM, Erdi Y, Akhurst T, et al. Tumor treatment response based on visual and quantitative changes in global tumor glycolysis using PET-FDG imaging: the Visual Response Score and the change in total lesion glycolysis. Clin Positron Imaging 1999;2(3):159–171.
55. Nair N, Ali A, Green AA, et al. Response of osteosarcoma to chemotherapy: evaluation with F-18 FDG-PET scans. Clin Positron Imaging 2000;3: 79–83.
56. Ma LD, Frassica FJ, Scott WW, et al. Differentiation of benign and malignant musculoskeletal tumors: potential pitfalls with MR imaging. Radiographics 1995;15:349–366.
57. Garcia R, Kim EE, Wong FC, et al. Comparison of fluorine-18–FDG PET and technetium-99m-MIBI SPECT in evaluation of musculoskeletal sarcomas. J Nucl Med 1996;37(9):1476–1479.
58. el-Zeftawy H, Heiba SI, Jana S, et al. Role of repeated F-18 fluorodeoxyglucose imaging in management of patients with bone and soft tissue sarcoma. Cancer Biother Radiopharm 2001;16(1):37–46.
59. Fletcher BD. Imaging pediatric bone sarcomas: diagnosis and treatment related issues. Radiol Clin North Am 1997;35:1477–1494.
60. Hains SF, O'Doherty MJ, Lucas JD, Smith MA. Fluorodeoxyglucose PET in the evaluation of amputations for soft tissue sarcoma. Nucl Med Commun 1999;20(9):845–848.
61. Blau M, Nagler W, Bender MA. Fluorine-18: a new isotope for bone scanning. J Nucl Med 1962;3:332–334.
62. Schiepers C, Nuyts J, Bormans G, et al. Fluoride kinetics of the axial skeleton measured in vivo with fluorine-18–fluoride PET. J Nucl Med 1997; 38(12):1970–1976.
63. Hoh CK, Hawkins RA, Dahlbom M, et al. Whole body skeletal imaging with [18F]fluoride ion and PET. J Comput Assist Tomogr 1993;17(1):34–41.
64. Cook GJ, Fogelman I. Detection of bone metastases in cancer patients by 18F-fluoride and 18F-fluorodeoxyglucose positron emission tomography. Q J Nucl Med 2001;45(1):47–52.
65. Schirrmeister H, Guhlmann A, Kotzerke J, et al. Early detection and accurate description of extent of metastatic bone disease in breast cancer with fluoride ion and positron emission tomography. J Clin Oncol 1999; 17(8):2381–2389.
66. Schirrmeister H, Glatting G, Hetzel J, et al. Prospective evaluation of the clinical value of planar bone scans, SPECT, and (18)F-labeled NaF PET in newly diagnosed lung cancer. J Nucl Med 2001;42(12):1800–1804.
67. Schirrmeister H, Guhlmann A, Elsner K, et al. Sensitivity in detecting osseous lesions depends on anatomic localization: planar bone scintigraphy versus 18F PET. J Nucl Med 1999;40(10):1623–1629.
68. Even-Sapir E, Metser U, Flusser G, et al. Assessment of malignant skeletal disease: initial experience with 18F-fluoride PET/CT and comparison

between 18F-fluoride PET and 18F-fluoride PET/CT. J Nucl Med 2004; 45(2):272–278.
69. Jager PL, Franssen EJ, Kool W, et al. Feasibility of tumor imaging using L-3–[iodine-123]-iodo-alpha-methyl-tyrosine in extracranial tumors. J Nucl Med 1998;39(10):1736–1743.
70. Tomiyoshi K, Amed K, Muhammad S, et al. Synthesis of isomers of ^{18}F-labelled amino acid radiopharmaceutical: position 2- and 3-L-^{18}F-alpha-methyltyrosine using a separation and purification system. Nucl Med Commun 1997;18(169):175.
71. Watanabe H, Inoue T, Shinozaki T, et al. PET imaging of musculoskeletal tumours with fluorine-18 alpha-methyltyrosine: comparison with fluorine-18 fluorodeoxyglucose PET. Eur J Nucl Med 2000;27(10):1509–1517.
72. Been LB, Suurmeijer AJH, Cobben DCP, et al. [F18]FLT-PET in oncology: current status and opportunities. Eur J Nucl Med Mol Imaging 2004; 31:1659–1672.
73. Cobben DC, Elsinga PH, Suurmeijer AJH, et al. Detection and grading of soft tissue sarcomas of the extremities with (18)F-fluoro-3′-deoxy-L-thymidine. Clin Cancer Res 2004;10:1685–1690.
74. Ishiwata K, Enomoto K, Sasaki T, et al. A feasibility study on L-[1-carbon-11]tyrosine and L-[methyl-carbon-11]methionine to assess liver protein synthesis by PET. J Nucl Med 1996;37(2):279–285.
75. Inoue T, Kim EE, Wong FC, et al. Comparison of fluorine-18-fluorodeoxyglucose and carbon-11-methionine PET in detection of malignant tumors. J Nucl Med 1996;37(9):1472–1476.
76. Hara T, Yuasa M. Automated synthesis of [11C]choline, a positron-emitting tracer for tumor imaging. Appl Radiat Isotopes 1999;50(3):531–533.
77. Yanagawa T, Watanabe H, Inoue T, et al. Carbon-11 choline positron emission tomography in musculoskeletal tumors: comparison with fluorine-18 fluorodeoxyglucose positron emission tomography. J Comput Assist Tomogr 2003;27(2):175–182.
78. Zhang H, Tian M, Oriuchi N, et al. 11C-choline PET for the detection of bone and soft tissue tumours in comparison with FDG PET. Nucl Med Commun 2003;24(3):273–279.
79. De Grado TR, Coleman RE, Wang S, et al. Synthesis and evaluation of ^{18}F-labelled choline as an oncologic tracer for positron emission tomography: initial findings in prostate cancer. Cancer Res 2001;61:110–117.